The Studies on the Various Crystalline-State Reactions and Their Molecular Dynamic Behavior by the X-ray Structure Analysis

（X線構造解析による種々の結晶相反応とその分子動的挙動に関する研究）

MOCHIZUKI EIKO

OSAKA UNIVERSITY

2001

Preface

The present works were carried out under the guidance of professor Yasushi Kai, Department of Materials Chemistry, Graduate School of Engineering, Osaka University, Japan, from 1995 to 2000.

The interest of this study is focused on the relationship between structure, reactivity and mechanism in the crystal phase reaction. The results and findings obtained through this worok gave important infprmation on the crystal phase reaction.

This fundamental work is expected to contribute to further developent on the technique of X-ray structure analysis.

Mochizuki Eiko

Department of Materials Chemistry
Graduate School of Engineering
Osaka University
Yamadaoka2-1, Suita
Osaka 565-0871
Japan

November, 2001

Contents

Chapter 4

Single-Crystal-to-Single-Crystal Enantioselective [2+2] Photodimerization of Coumarin, Thiocoumarin and Cyclohex-2-enone in the Inclusion Complexes with Chiral Host Compounds

General Introduction

Molecules in a crystal are regularly arranged close to each other, and afford a unique three-dimensional interaction field. Because the molecular interaction field is assembled in an orderly state, a chemical reaction between the packed molecules in a crystalline phase can be expected to progress more efficiently and selectively than that in a solution. Moreover, a specific chemical reaction which does not be achieved in solution can proceed in a crystalline phase.

A high-efficient and high-selective crystalline-state reaction will occur between the molecules restricted in a crystal lattice by external triggers, such as temperature, light irradiation, pressure, electric field, and magnetic field , or a combination of these factors. The reaction gives new organic crystalline materials which have high electronic conductivity or good optical properties, for example .

It has been observed that when a chemical reaction occur in a crystalline phase, these are some cases that the crystal maintains its original form[1]. A recently developed rapid X-ray diffractometer enables us to observe a molecular dynamic behavior in a crystalline phase. This rapid X-ray diffractometer is different from the conventional four-circle diffractometer because it has high-sensitive two-dimensional detector called *imaging plate.* We can analyze the mechanism of the reaction mentioned above using the X-ray diffractometer.

It is very important to clarify the changes in dynamic structures of arranged molecules caused by a reaction in a crystalline phase. Additionally, the changes in physical and chemical properties before and after the reaction and the exploration of new functions induced by the reaction will be worthy of remark. Detailed studies in such the structure and function correlation will enable us not only to design the three-dimensional interaction field but also to innovate

a new field of the solid organic chemistry which is different from the current organic chemistry in solution. Some molecular assemblies with the required reactivity and property will be afforded by using such a controlled three-dimensional interaction field.

The aim of this study is to analyze the mechanism of molecular reactions in solid phase by using the X-ray structure analysis.

This thesis consists of the following four chapters.

Chapter 1 describes the crystal structures and the solid-state polymerization of the bifunctional derivatives having diacetylene moieties. The crystallographic analysis was undertaken to elucidate the contribution of the two functional groups to the polymerization.

Chapter 2 deals with a detailed study concerning the crystal structures of a series of 1-alkylthymine homologues (carbon numbers of the alkyl chain were 8,11,12,13,14, and 16)based on the X-ray crystal analysis.

Chapter 3 shows that crystal structure and photodimerization of 1-alkylthymine were studied in a single crystals. 1-Alkylthymine gave two types of crystals, depending both on the length of alkyl chains and solvent used.

Chapter 4 describes the unique single-crystal-to-single-crystal enantioselective [2+2] photodimerization reactions of inclusion complexes derived from coumarin, thiocoumarin, and cyclohex-2-enone . These three substrates formed the corresponding inclusion complexes with (*R,R*)-(-)-*trans*-bis(hydroxydiphenylmethyl)-2,2-dimethyl-1,3-dioxacyclopentane, (*R,R*)-(-)-*trans*-2,3-bis(hydroxydiphenylmethyl)-1,4-dioxaspiro[4.4]nonane, and (-)-1,4-bis[3-(o-chlorophenyl)-3-hydroxy-3-phenylprop-1-ynyl]benzene, respectively. The single-crystal-to-single-crystal nature and the steric course of them were investigated by the X-ray crystallographic analysis and X-ray powder diffraction spectroscopy.

1) V. Enkelmann, *Adv. Polym. Sci.*, **63**, 91 (1984).

Chapter 1

Crystal Structures and Solid-state Reactivities of 1,4- and 1,2-Bis(5-hydroxypenta-1,3-diynyl)benzenes and 1-(5-hydroxypenta-1,3-diynyl)-4-ethynylbenzene

1-1 Introduction

The author's group have previously reported on the reactions of γ-irradiated crystals of diethynylbenzene derivatives.[1-3] The crystal structures of the monomers were definitely affected by the nature of the substituents and their positions in the aromatic ring, leading to a variety of solid-state reactivities. Polymerization or dimerization occurred selectively depending on the crystal structures in contrast to the non-selective reactivities in solution. The present study is concerned with the crystal structures and the solid-state polymerization of the bifunctional derivatives having diacetylene moieties. The structures and the melting points of the monomers, 1,4-bis(5-hydroxypenta-1,3-diynyl)benzene (**1**), 1,2-bis(5-hydroxypenta-1,3-diynyl)-benzene (**2**) and 1-(5-hydroxypenta-1,3-diynyl)-4-ethynylbenzene (**3**), used in the present study, are shown in Fig. 1.

Solid-state polymerization of diacetylene derivatives has been extensively studied in connection with both of the propagation processes and the properties of π-conjugation of the product polymers including nonlinear optical properties.[4,5] Recently, attempting the enhancement of the π-conjugation properties, bifunctional diacetylene monomers and octatetraynes have been synthesized and their polymerization reactivities have been investigated.[7-14] The radiation-induced solid-state polymerization has been reported for 1,4-bis(1,3-octadecadiynyl)benzene, an analogue of **1**. However, there has been no report on the crystal structures of the bifunctional diacetylene monomers. In the present study the crystallographic analysis was undertaken to elucidate the contribution of the two functional groups to the polymerization.

The crystal structure of **1** depended on recrystallization solvents. Changes in the recrystallization conditions of **1** revealed that it exists in two crystalline forms, designated as **1a** and **1b**.

1

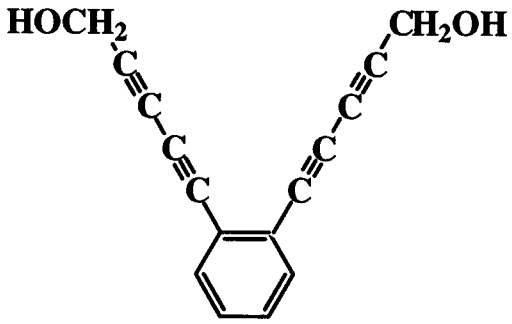

2: mp 135.2-136.0°C

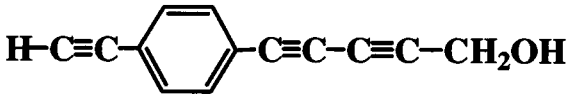

3: mp 139.4-140.3°C

Fig. 1. Structures of monomers.

The **1a** crystals were obtained from acetone-benzene mixtures and the **1b** crystals, from pure acetone. Upon γ-irradiation, **1a** polymerized to be insoluble in common organic solvents. Polymers were obtained neither from **1b**, nor from the crystals of **2**. The reactivities in polymerization are correlated to the monomer packings in the crystals. The polymerization was also examined for **3**.

1-2 Experimentals

Polymerization experiments

The monomers, **1** and **3**, were prepared by the coupling of 1,4-diethynylbenzene and 3-bromopropyn-1-ol by the literature method[15] and were purified by repeated recrystallization. Similarly, **2** was prepared from 1,2-diethynylbenzene and 3-bromopropyn-1-ol and was recrystallized. The diethynylbenzenes were prepared from 1,2- and 1,4-diiodobenzenes (Aldrich and Wako Chemicals, respectively) according to the literature.[16] 3-Bromo-propyn-1-ol was

prepared according to the literature.[17] The monomer crystals were sealed in Pyrex tubes under vacuum and were irradiated at room temperature with γ-rays from a ^{60}Co source at a dose rate of 5.2 kGy h^{-1} (1 Gy = 1 J kg^{-1}). The polymer conversions were determined by comparison of the relative intensities of the stretching bands of the corresponding carbon-carbon triple bonds, –C ≡ C-H (3263 cm^{-1}) and -C ≡ C–C ≡ C- (2240 cm^{-1}), with those of the aromatic rings (832 cm^{-1}) of the FTIR spectra (KBr) of the original and irradiated crystals. The FTIR spectra were recorded on a Perkin Elmer Spectrum 2000 spectrophotometer. Fig. 2 shows the FTIR spectra of the original crystals of **1a** and **3**, which polymerized upon γ-irradiation or heating.

Gel permeation chromatographic measurement was carried out by 262-nm absorption in tetrahydrofuran using Shimadzu CR3A equipped with two 30-cm TSK-Gel G6000PWXL and G3000PWXL columns connected in series.

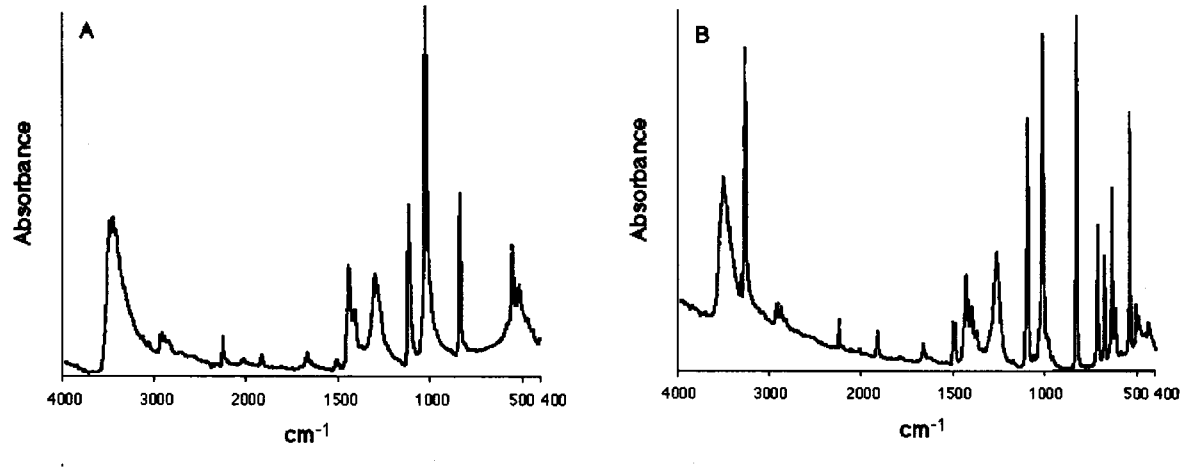

Fig. 2. FTIR spectra of the original crystals of (A) **1a** and (B) **3**.

X-ray crystal structure analysis

The crystal data and experimental details are summarized in Table 1. X-ray diffraction data were collected by a Rigaku AFC-5R diffractometer with graphite-monochromated Cu-$K\alpha$ radiation (λ= 1.54178 Å) up to $2\theta_{max}$ of 120.1°. All the crystallographic calculations were

carried out by using TEXSAN software package of the Molecular Structure Corporation. The crystal structures were solved by the direct method and were refined by the full-matrix least-squares. All the non-hydrogen atoms and hydrogen atoms were refined anisotropically and isotropically, respectively.

Full crystallographic details (excluding structure factors) for the structures reported in this paper have been deposited with the Cambridge Crystallographic Data Centre (CCDC). For

Table 1. Crystal Data and Experimental Conditions

Parameter	**1a**	**1b**	**2**	**3**
Empirical Formula	$C_{16}H_{10}O_2$	$C_{16}H_{10}O_2$	$C_{16}H_{10}O_2$	$C_{13}H_8O$
Formula Weight	234.25	234.25	234.25	180.21
Crystal dimension /mm	0.30x0.25x0.10	0.30x0.20x0.20	0.30x0.30x0.25	0.40x0.30x0.15
Crystal System	monoclinic	monoclinic	monoclinic	monoclinic
Space Group	$P\,2_1/c$	$C\,2/c$	$P\,2_1/n$	$P\,2_1$
a / Å	4.104(3)	17.669(3)	8.179(2)	4.041(1)
b / Å	5.427(6)	8.058(3)	8.826(3)	5.641(3)
c / Å	26.816(2)	9.354(3)	17.338(2)	21.062(4)
β / °	94.07(6)	115.76(2)	94.15(1)	93.16(2)
V / Å^3	595.8(8)	1199.5(5)	1248.2(5)	479.3(3)
Z	**2**	**4**	**4**	**2**
d_{calcd} / g cm^{-3}	1.306	1.297	1.246	1.248
μ(Cu$K\alpha$) / cm^{-1}	6.90			
μ(Mo$K\alpha$) / cm^{-1}		0.79	0.76	0.78
F(000)	244.00	488.00	488.00	188.00
No. of Reflections, m with (I> 2σ(I))	642	773	1719	911
No. of variable, n	103	107	204	160
R [a)]	0.042	0.060	0.050	0.040
Rw [b)]	0.049	0.066	0.049	0.042
GOF [c)]	3.32	1.51	1.69	1.59
$\Delta\rho_{max}$ /eÅ^{-3}	0.14	0.18	0.16	0.10

a) $R = \Sigma\,(|F_o|-|F_c|) / \Sigma\,|F_o|$ b) $Rw = [\,\Sigma\omega\,(|F_o|-|F_c|)^2 / \Sigma\omega\,|F_o|^2]^{1/2}$ c) $GOF = [\Sigma\omega\,(|F_o|-|F_c|)^2 /(m-n)]^{1/2}$
Diffractometer : Rigaku AFC-5R Crystal Structure Analysis : teXsan
Structure Solution : Direct Method (Shelxs86)
Refinement : Full-matrix least-squaresirect Method (Shelxs86)
Refinement : Full-matrix least-squares

details of the deposition scheme, see 'Instructions for Authors', *J. Chem. Soc., Perkin Trans. 2*, available via the RSC Web page (http://www.rsc.org/authors). Any request to the CCDC for this material should quote the full literature citation and the reference number.

1-3 Results and Discussion

Upon heating, the **1a** crystals, obtained from acetone-benzene mixtures, turned black above *ca.* 120°C and did not melt beyond 300°C. When recrystallized from pure acetone, the colouration of the crystals, **1b**, was observed to begin at *ca* 160°C, and the black crystals melted at 210°C. Thus, the melting point was not determined for the crystals of **1** because of the occurrence of polymerization upon heating. The crystal structure of **1** depends on the recrystallization solvents. Fig. 3 shows the crystal structure of **1a**. The diacetylene groups were arranged regularly along the *b* axis. The regular arrangement along the *b* axis is formed by the hydrogen bonding between the neighbouring hydroxyl groups.

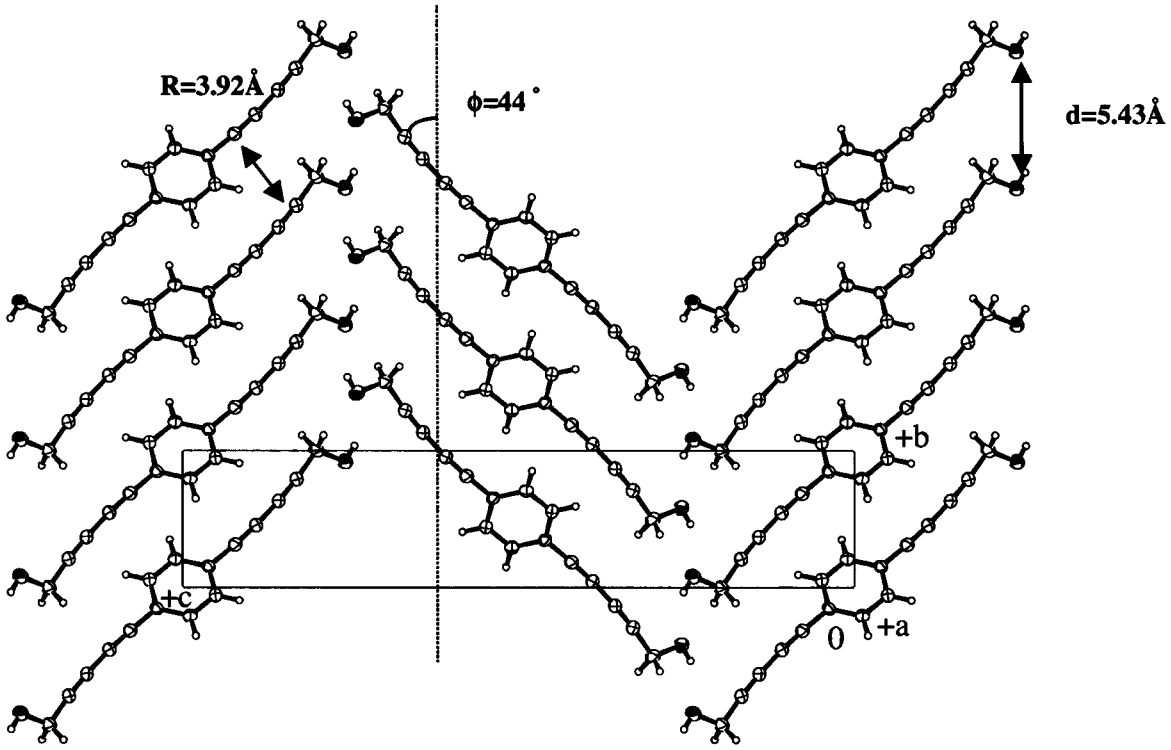

Fig.3 Crystal structure of **1** recrystallized from acetone-benzene mixtures viewed down the *a* axis.

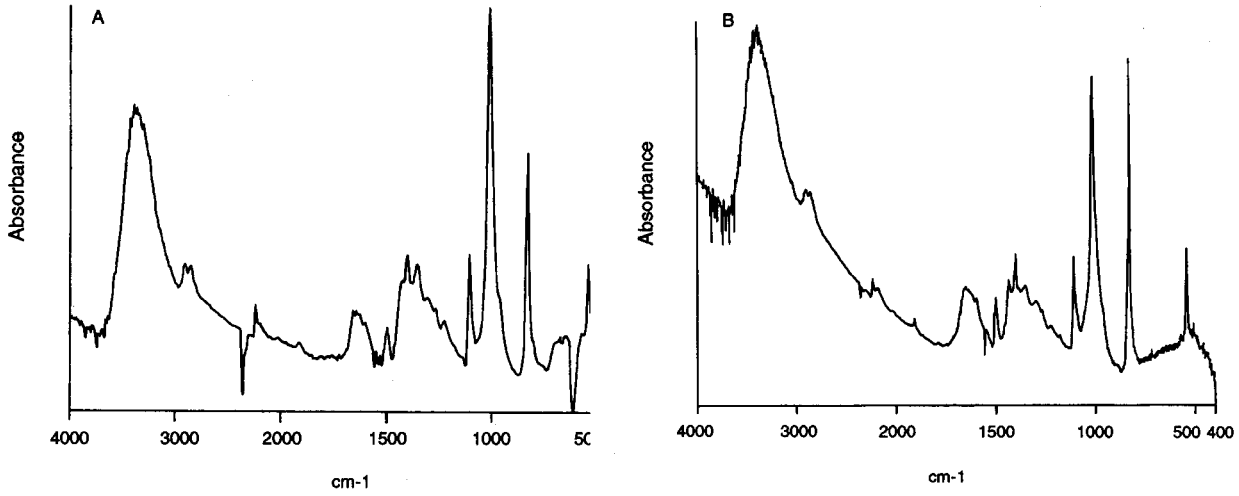

Fig. 4 FTIR spectra of **1a** (A) irradiated at a dose of 2.0 MGy and (B) heated at 100℃ for 25 h.

To define the arrangement of diacetylene monomers, the following parameters are used.[6] They are the intermolecular distance, R, between the reacting carbons, the stacking distance, d, between the neighbouring monomers and the angle, ϕ, between diacetylene rod and stacking axis. In the crystal structure of **1a**, R, d and ϕ are 3.92 Å, 5.43 Å and 44°, respectively; these parameters are in the range[6] reported to be favorable for the polymerization.[6] Thus, the solid-state polymerization in this crystal is considered to proceed along the *b* axis. The **1a** crystals polymerized to be insoluble in common organic solvents when irradiated with γ-rays or heated

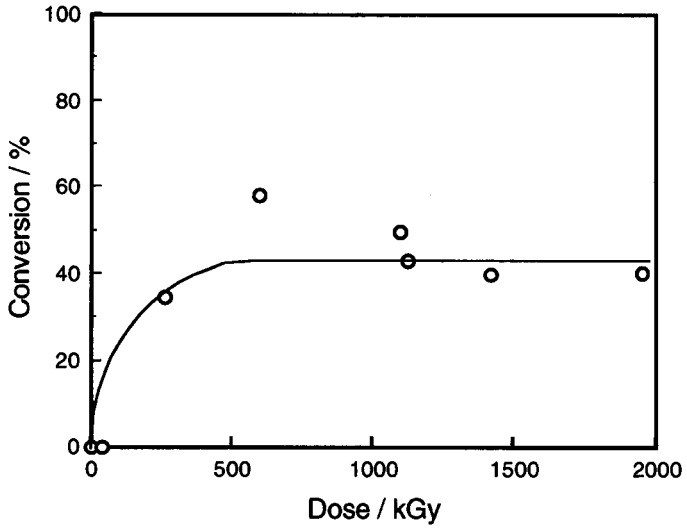

Fig. 5 Dose-conversion curve for the radiation induced polymerization of **1**, obtained from acetone-benzene mixtures.

and the colourless crystals became black, as expected from the crystal data. Fig. 4 shows the FTIR spectra of **1a,** irradiated with γ rays at a dose of 2.0 MGy and heated at 100°C for 25 h. The absorption intensity of the -C ≡ C–C ≡ C- band at 2240 cm^{-1} decreases and a new band appears at around 2190 cm^{-1}, which is assigned to conjugated acetylene.[8] Fig. 5 shows the dose-conversion curve for the radiation-induced polymerization of **1a**. The conversion seems to be constant at below 50% above the irradiation dose of *ca.* 500 kGy. There was no appreciable change in the FTIR spectra at the high irradiation doses. least above 1.0 MGy. Therefore, the radiation-induced polymerization is considered to proceed by one of the diacetylene moieties. Fig. 6 shows the time-conversion curves for the thermal polymerization at 100 and 150°C. It is

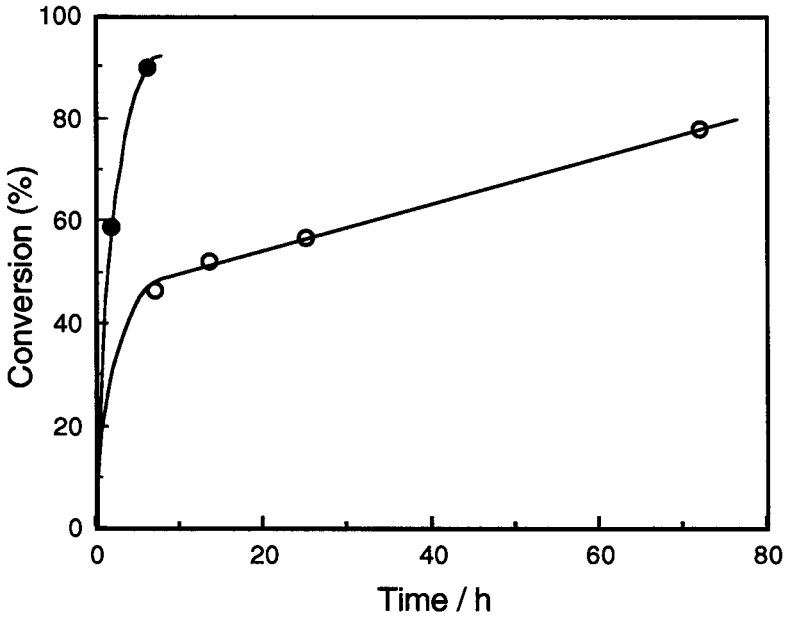

Fig. 6 Time-conversion curves for the thermal polymerization of **1**, obtained from acetone-benzene mixtures, at (○) 100 and (●) 150°C.

demonstrated that the both acetylene moieties participate in the thermal polymerization, resulting in the conversion above 50%. The FTIR spectral change around the 2240- and 2190-cm^{-1} bands at 100°C is illustrated in Fig. 7.

Fig. 8 shows the crystal structure of **1b.** It was found that the arrangement of the aromatic rings in the neighbouring monomer molecules is not parallel. The parameters of R, d and ϕ are 6.08 Å, 9.35 Å and 24°, respectively, and indicate that the arrangement of this crystal is not

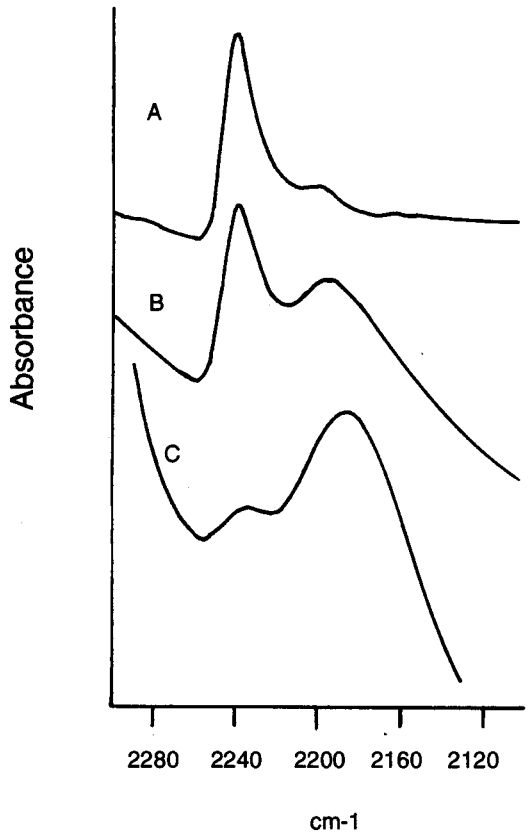

Fig. 7 Change in the absorption intensities of the 2240- and 2190-cm^{-1} bands the **1 a** crystals upon heating at 100℃: the heating times are A, 0 h; B, 25 h; and C, 72 h.

hydroxyl groups. On the other hand, from the crystal packing projected along the *b* axis, it was found that the ethynyl moieties are regularly arranged along the *a* axis and the shortest carbon-carbon distance of the neighboruing ethynyl moieties is 3.79 Å (Fig. 10b). On the basis of the molecular arrangement, the solid-state polymerization of **3** by the ethynyl moiety is expected to proceed, similarly to the case of 1,4-diethynylbenzene.[1] Thus, with respect to the crystals of **3**, the monomer arrangement is suitable for the solid-state polymerization not only by the diacetylene moieties but also by the ethynyl groups. The distance between the reacting carbons is shorter for the ethynyl groups than for the diacetylene moieties. So the polymerization is expected to be preferable for the ethynyl groups than for the diacetylene moieties. A short time irradiation of the crystals of **3** resulted in a poor crystallinity. This may be due to the scission of the hydrogen bonds between the neighbouring diacetylene moieties caused by the predominant bond formation between the ethynyl groups. Such a lowering of the crystallinity was not observed for the

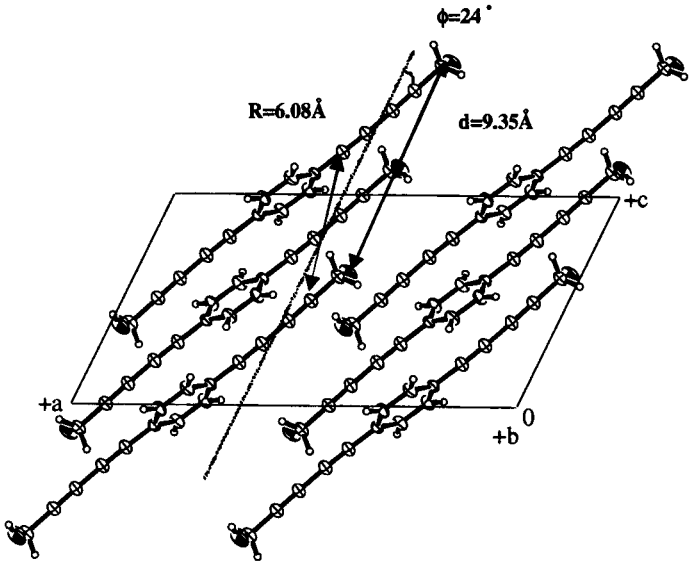

Fig. 8 Crystal structure of **1** recrystallized from acetone viewed down the *b* axis

suitable for the polymerization. The crystals did not polymerize upon γ-irradiation as expected. The **Ib** crystals irradiated at a dose of 510 kGy was submitted to gel permeation chromatography. Even low molecular weight oligomers were not detected by the gel permeation chromatogram of the irradiated crystals. Neither polymerized **1b** upon heating at 150°C and below.

No crystals polymerizable upon γ-irradiation and heating were obtained from **2**. The melting point of the crystals obtained from ethyl acetate was 135.2-136.0°C. Fig. 9 shows the structure of the inert crystals. The parameters of R, d and ϕ are 6.19 Å, 8.83 Å and 34°, respectively,

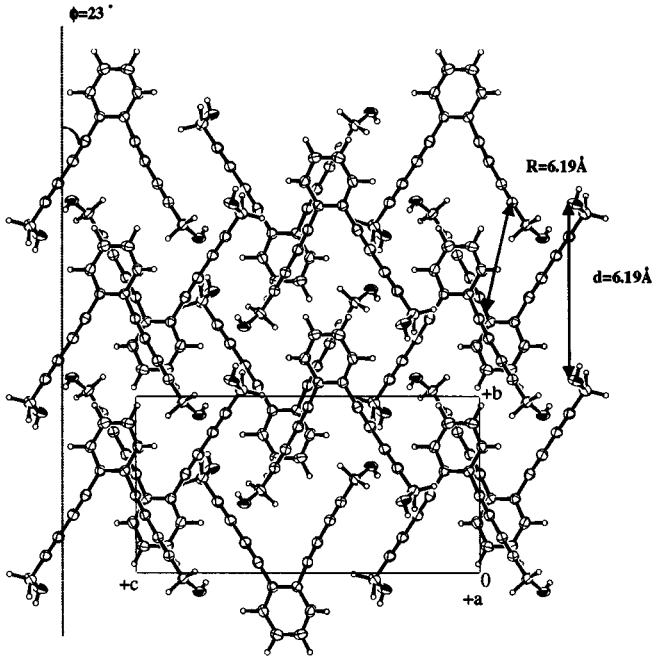

Fig. 9 Crystal structure of **2** viewed down the *a* axis.

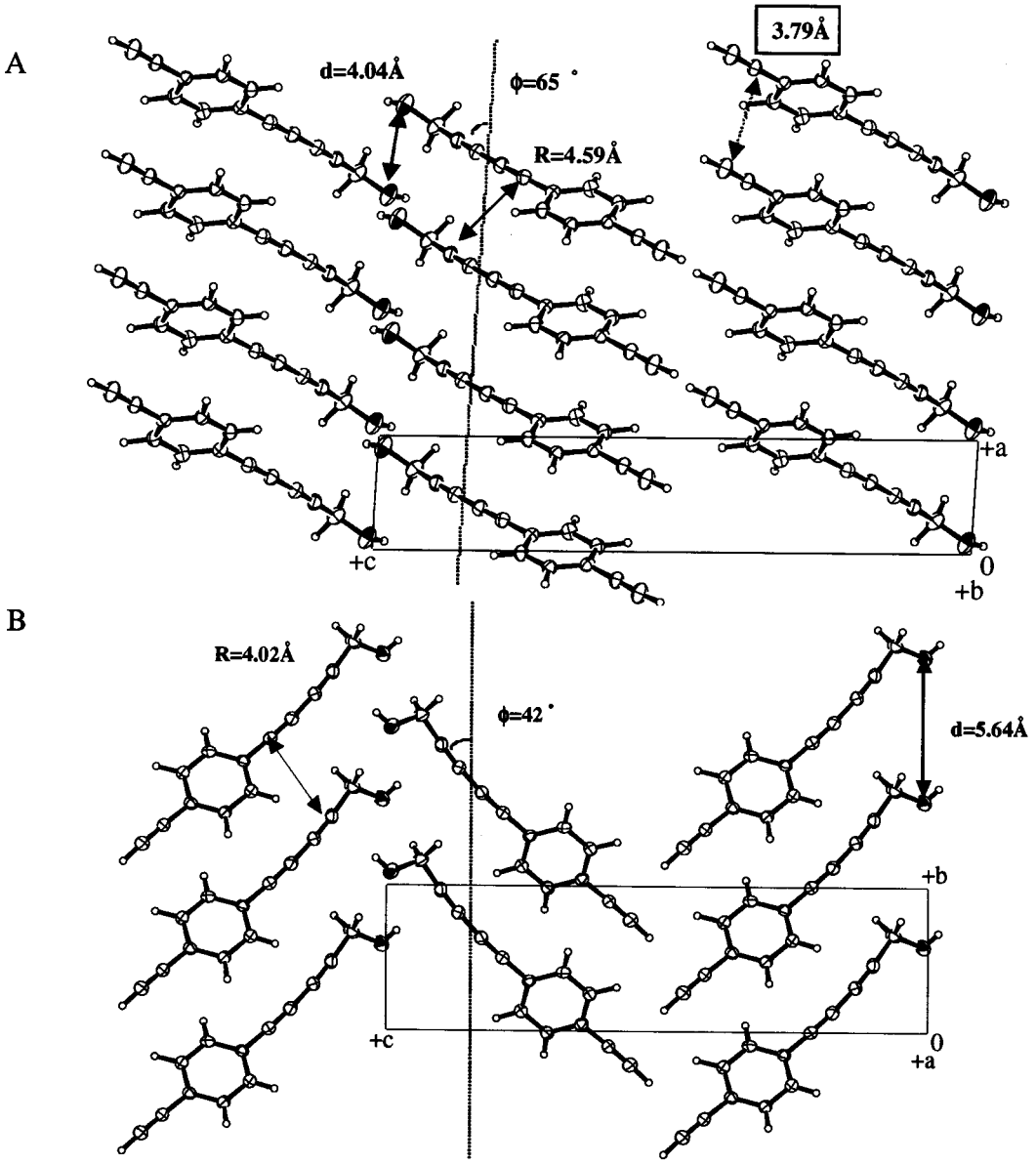

Fig. 10 Crystal structure of **3** viewed down the (A) *a* and (B) *b* axes.

which indicate the arrangement of crystal **2** is unfavorable for the polymerization.[6]

Figs. 10a and 10b show the crystal structure of **3**, obtained from hexane-acetone mixtures. Considering from the *a* axis projection of the crystal packing style, the diacetylene groups are arranged along the *b* axis and their packing parameters R, d and ϕ are 4.02 Å, 5.64 Å and 42°, respectively (Fig. 10a). It was found that this crystal structure is quite similar to the crystal structure of **1a** and the crystals of **3** take suitable packing structures for the solid-state polymerization. Therefore, it is expected that this monomer is polymerized along the *b* axis. The regular arrangement along the *b* axis is also formed by the hydrogen bonding between the neighbouring

irradiated **1a** crystals, where the crystal lattice is held by the diacetylene polymerization.

The crystals of **3** polymerize upon γ-irradiation but not upon heating. A decrease in absorption intensity at 2240 cm^{-1} was observed in the FTIR spectra of the irradiated crystals of **3** as well as an appearance of a new band at 2190 cm^{-1}, similarly to the case of **1a**. In addition, the absorption intensity of the -C≡C-H band at 3263 cm^{-1} decreased by the γ-irradiation. Thus, both of the ethynyl and butadiynyl groups participate in the polymerization, as expected from the crystallographic data. Fig. 11 shows the dose-conversion curves for the radiation-induced polymerization of **3**. The conversion of the ethynyl group is higher than that of the butadiynyl group. Furthermore, the conversion of the butadiynyl group of **3** is lower than that of **1a**. These results can be interpreted in terms of the relatively long distance between the reacting carbons of the butadiynyl group of **3**, 4.04 Å. The polymerization by the butadiynyl group may have an induction period (Fig. 11), although there may be some errors in the low yields in the early stage of the polymerization. On the basis of the molecular arrangement of the crystals, the two propagations by the ethynyl and butadiynyl groups of **3** are considered to proceed along the

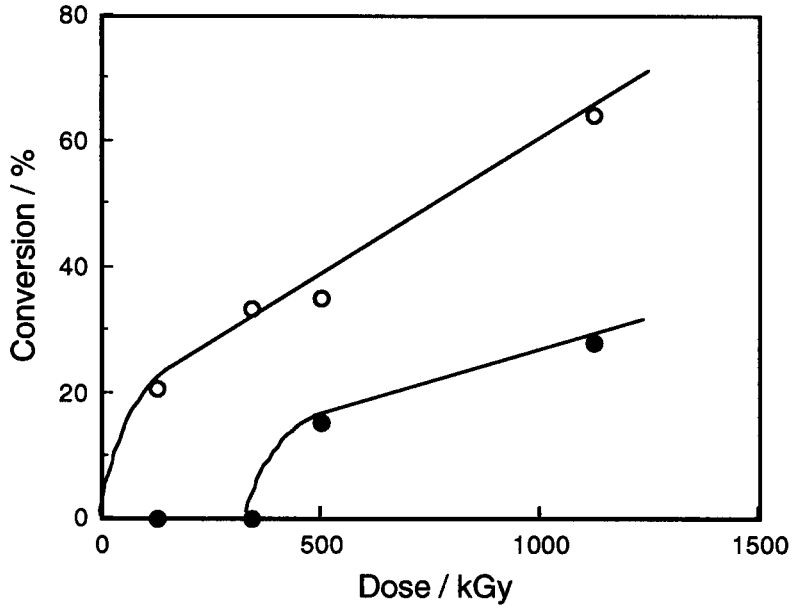

Fig. 11 Dose-conversion curve for the radiation-induced polymerization of **3** by the (○) ethynyl and (●) butadiynyl groups.

different axes of the crystals.

The relatively long distance between the reacting carbons of the butadiynyl group of **3** may be responsible for the inertness toward heating. The ethynyl group may also be inert toward heating. In our previous study,[1] 1,4-diethynylbenzene did not polymerize upon heating below the melting point, 94-95°C, whereas it polymerized upon irradiation with γ-rays[1] and UV light.[18] The ethynyl groups attached to aromatic rings are considered to be inert in the thermal polymerization in crystalline states, since the melting points of various aromatic acetylenes have been determined.[18]

1-4 Conclusion

Crystal structures and the solid-state polymerization of 1,4-bis(5-hydroxypenta-1,3-diynyl)benzene (**1**), 1,2-bis(5-hydroxypenta-1,3-diynyl)benzene (**2**) and 1-(5-hydroxypenta-1,3-diynyl)-4-ethynylbenzene (**3**) were investigated. The crystal structure of **1** depends on recrystallization solvents. The crystals obtained from acetone-benzene mixtures polymerize when irradiated with γ-rays or heated. The colourless crystals become black and insoluble in common organic solvents. Only one of the butadiynyl groups participates in the radiation-induced polymerization, whereas the both, in the thermal polymerization. Polymerization does not occur for the crystals obtained from pure acetone. The polymerization reactivities were correlated to the crystal structures. Polymerizable crystals were not obtained from **2**. The arrangement of the butadiynyl groups in the crystals of **2** is unfavorable for the polymerization. The crystals of **3**, obtained from hexane-acetone mixtures, polymerize upon γ-irradiation but not upon heating. In the radiation-induced polymerization of **3**, the propagation by the ethynyl and butadiynyl groups is considered to proceed independently along the different crystal axes. The ethynyl group is more reactive than the butadiynyl group because of the shorter intermolecular carbon-carbon distance responsible for the polymerization. The difference in reactivity toward heating between **1** and **3** may also be attributed to the intermolecular carbon-carbon distances of the butadiynyl groups.

1-5 References

1. M. Hagihara, Y. Yamamoto, S. Takahashi and K. Hayashi, *Radiat. Phys. Chem.*, 1986, **28**,165.
2. Y. Kai, A. Yamamoto, D. Xu, N. Kasai, M. Hagihara, Y. Yamamoto, S. Takahashi and K.Hayashi, *Makromol. Chem.*, 1987, **188**, 3047.
3. Y. Yamamoto, T. Ueda, N. Kanehisa, K. Miyawaki, Y. Takai, S. Tagawa, M. Sawada and Y.Kai., *J. Chem. Soc., Perkin Trans. 2*, **1997**, 734.
4. H. Basseler, *Adv. Polym. Sci.*, 1984, **63**, 1.
5. H. Sixl, *Adv.Polym. Sci.*, 1984, **63**, 49.
6. V. Enkelmann, *Adv. Polym. Sci.*, 1984, **63**, 91.
7. S. Okada, H. Matsuda, A. Masaki, H. Nakanishi and K. Hayamizu, *Chem. Lett.*, **1997**, 1105.
8. S. Okada, H. Matsuda, H. Nakanishi and M. Kato, *Mol. Cryst. Liq. Cryst.*, 1990, **189**, 57.
9. S. Okada, K. Hayamizu, H. Matsuda, A. Masaki and H. Nakanishi, *Bull. Chem. Soc. Jpn.*, 1991, **64**, 857.
10. S. Okada, K. Hayamizu, H. Matsuda, A. Masaki, N. Minami and H. Nakanishi, *Macromolecules*, 1994, **27**, 6259.
11. K. Hayamizu, S. Okada, T. Doi, H. Kawanami, N. Kikuchi, H. Matsuda and H. Nakanishi, *Bull. Chem. Soc. Jpn.*, 1995, **68**, 791.
12. S. Nezu and J. B. Lando, *J. Polym. Sci.: Part A: Polym. Chem.*, 1995, **33**, 2455.
13. W. S. Price, N. Kikuchi, H. Matsuda, K. Hayamizu, S. Okada and H. Nakanishi, *Macromolecules*, 1995, **28**, 5363.
14. H. Matsuzawa, S. Okada, H. Matsuda and H. Nakanishi, *Chem. Lett.*, **1997**, 1105.
15. L. Brandsma, *Preparative Acetylenic Chemistry*, Elsevier, Amsterdam, 1988, ch. 10, p. 212.
16. S. Takahashi, Y. Kuroyama, K. Sonogashira and N. Hagihara, *Synthesis*, **1980**, 627.
17. T. Ando, S. Shioi and M. Nakagawa, *Bull. Chem. Soc. Jpn.*, 1972, **45**, 2611.
18. O. Rohde and G. Wegner, *Makromol. Chem.*, 1978, **179**, 2013.

Chapter 2

Structures and Photodimerizations of 1-Alkylthymine Crystals Obtained from *N, N*-Dimethylformamide

2-1 Introduction

The photodimerization of thymine derivatives in solution is known to give four kinds of isomers as the photodimers by UV irradiation at 280 nm.[1] In the case of the photoreaction of DNA, the isomer of the cyclobutane type photodimer obtained was only *cis-syn* photodimer.[2] The stereoselective photodimerization of thymine bases in DNA occurred under the control of polymer chain and the hydrogen bonding with adenine bases. Therefore, the stereoselective photodimerization can be expected for the thymine base in single crystal under the control of crystal lattice.

The photodimerization of thymine compounds is reversible and is applicable to photoresists[3, 4, 5, 6, 7] and reversible photo-recording systems[8, 9, 10, 11, 12] In order to apply the thymine compounds to photosensitive materials, it is necessary to study the photodimerization reactions in solid state. For a highly efficient reversible photodimerization system of the thymine compounds, the stereoselective photodimerization is an important factor, because the splitting reaction of the photodimer depends on the kinds of stereo isomer of the photodimer. The studies of the crystal structure and the photodimerization of the thymine derivatives will make the mechanism of the photodimerization clear for the solid state reaction.

We have recently reported that 1-octylthymine (Fig. 1) in single crystal obtained from ethyl acetate solution undergoes photodimerization when irradiated at 280 nm to form *trans-anti* photodimer (Fig. 2).[13] The X-ray structure analysis of 1-octylthymine crystal obtained from ethyl acetate solution (**Form I**) showed the thymine rings to be lying in *trans-syn* arrangement to each other. The arrangement of the thymine rings is such that the photodimer

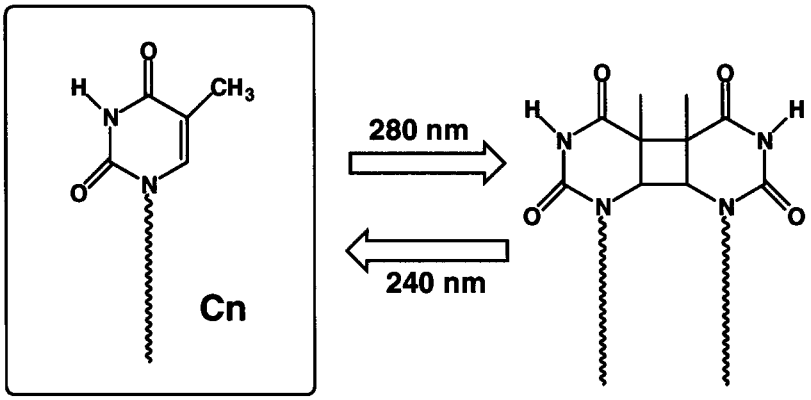

Fig.1 Reversible photodimerization of 1-alkylthymine.

resulting from irradiation of the crystal would be expected to attain *trans-syn* geometry. The isomer of the photodimer obtained from the crystal was not the *trans-syn* but the *trans-anti* photodimer. The *trans-anti* photodimer of the 1-octylthymine was concluded to be formed by disrotatory motion in the crystal during the photodimerization reaction (Fig. 2).

The plates of 1-octylthymine were obtained from ethanol solution (**Form II**), but the crystal did not undergo photodimerization by UV irradiation at 280 nm.[14] The X-ray structure analysis of the plates of 1-octylthymine showed that the crystal structure of the **Form II** resembled that of the **Form I** obtained from ethyl acetate solution except for the packing of the long alkyl chains.

The third crystal of **Form III** of 1-octylthymine was obtained from acetonitrile solution

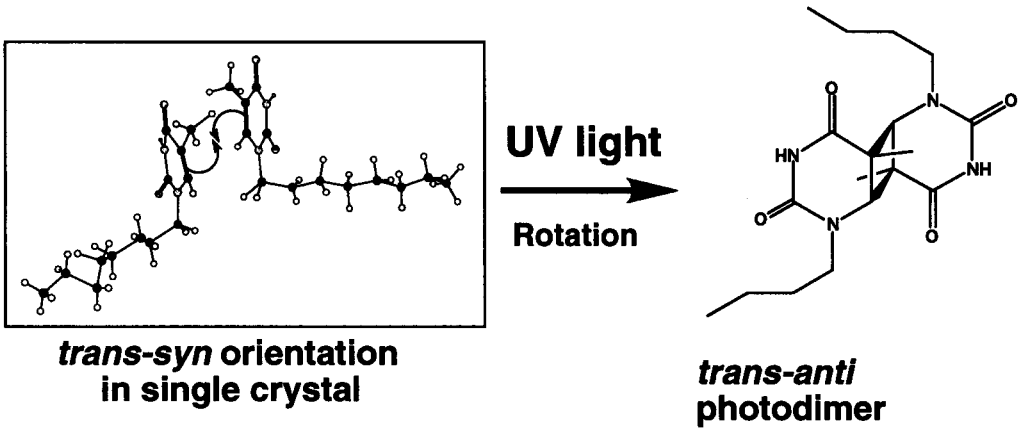

Fig. 2 Photodimerization of 1-octylthymine in single crystal.[13]

as needles.[15] The third crystal underwent photodimerization efficiently to form *trans-anti* and *trans-syn* photodimers. The thymine rings in the **Form III** were able to rotate during the photodimerization reaction to form two kinds of photodimers. In addition to 1-octylthymine, the crystal structure and the photodimerization of other 1-alkylthymines having long alkyl chains were studied for the needles obtained from acetonitrile. All these crystals have similar crystal structure and activity for the photodimerization. Polymorphism and photodimerization of 1-octylthymine are summarized for three crystal forms in Table 1.

Intensive studies concerning topochemical reactions have been reported on the photodimerization of cinnamic acid and its derivatives. Schmidt and his coworkers proposed a geometrical criterion for the photodimerization in the crystalline state: that the reacting double bonds should be situated within about 4.2 Å of each other and aligned parallel to each other.[16] In the case of the photoactive single crystal of 1-octylthymine obtained from acetonitrile solution (**Form III**), however, the distance between the reacting double bonds of the thymine bases was 4.47 Å.[15] It is difficult to apply Schmidt's rule to the photodimerization of the 1-octylthymine crystal. Therefore, it is necessary to determine the factor of the crystal structure of 1-alkylthymine for the photodimerization reaction in crystal state.

This paper deals with the structure of the 1-alkylthymine crystals (**Form IV**) obtained

Table 1 Polymorphism and photodimerization of 1-octylthymine.

Crystal Structure	Solvent	Shape	Photo-reaction	Isomers of Photodimer	Ref.
Form I	ethyl acetate, chloroform	plate	○	*trans-anti*	13)
Form II	ethanol, methanol, acetonitrile acetone	plate	×	-	14)
Form III	acetonitrile	needle	○	*trans-anti*, *trans-syn* (1:1)	15)

from *N, N*-dimethylformamide (DMF) solution, where the carbon numbers of the alkyl chain were 8, 11, 12, 13, 14, and 16. These crystals did not undergo photodimerization by UV irradiation at 280 nm. Then, the reason of inactivity for the photodimerization of the crystal from DMF was studied by comparing the crystal structure of 1-octylthymine with three forms (**Forms I**, **II**, and **III**) reported previously.

2-2 Experimentals

Materials

Preparations of the 1-alkylthymines are reported in our previous papers.[13, 14, 15] Solvents used for recrystallization were purified by a conventional method.

Instruments

Photodimerizations of the thymine bases in the single crystals (crystal size was around 0.5 x 0.2 x 0.05 mm) were carried out by SUPER CURE-203S UV, where the light source was a Hg-Xe lamp (200 W)(San-Ei Electric) with a cut filter (Toshiba U340).[15] The photodimerization was followed by measuring UV spectra (Nihon Bunko UV/VIS 600) in chloroform solution.

A Seiko I&E DSC6200 series performed differential scanning calorimetric (DSC) measurements. X-ray powder diffraction patterns were measured by a Rigaku X-ray diffractometer RINT 2000 with Cu-$K\alpha$ radiation.

Crystal Structure Analysis

Data of X-ray diffraction for 1-alkylthymine were collected by a Rigaku RAXIS-CS imaging plate two-dimensional area detector using graphite-monochromatized Mo-$K\alpha$ radiation (λ= 0.71070Å). Using TEXSAN software package of the Molecular Structure Corporation we performed all the crystallographic calculations. The crystal structures were solved by the direct methods (shelxs97) and refined by the full-matrix least squares. The positions of hydrogen atoms attached to nitrogen atoms were obtained from the difference Fourier syntheses. All non-hydrogen atoms and hydrogen atoms were refined anisotropically and

isotropically, respectively. The crystal data of six thymine derivatives are shown in Table 2.

Table 2 The crystal data of six 1-Alkylthymine derivatives.

alkyl	octyl (**C8**)	undecyl (**C11**)	dodecyl (**C12**)	tridecyl (**C13**)	tetradecyl (**C14**)	hexadecyl (**C16**)
solvent	DMF	DMF	DMF	DMF	benzene	benzene/*p*-xylene
formula	$C_{13}H_{22}N_2O_2$	$C_{16}H_{28}N_2O_2$	$C_{17}H_{30}N_2O_2$	$C_{18}H_{32}N_2O_2$	$C_{19}H_{34}N_2O_2$	$C_{21}H_{38}N_2O_2$
crystal system	monoclinic	monoclinic	monoclinic	monoclinic	monoclinic	monoclinic
space group	$P2_1/a$	$P2_1/a$	$P2_1/a$	$P2_1/a$	$P2_1/a$	$P2_1/a$
a / Å	12.405(4)	12.416(3)	12.416(3)	12.43(2)	12.424(7)	12.46(2)
b / Å	8.791(4)	8.884(5)	8.862(4)	8.921(3)	8.947(2)	8.972(7)
c / Å	16.87(1)	15.350(3)	18.17(2)	16.775(6)	18.234(6)	20.014(8)
α/ °						
β/ °	130.61(4)	96.51(2)	114.28(6)	90.88(6)	106.15(5)	100.27(7)
γ/ °						
V/ Å^3	1397(1)	1682.3(8)	1822(2)	1860(2)	1951(1)	2202(3)
Z	4	4	4	4	4	4
Dcalc /gcm^{-3}	1.13	1.11	1.07	1.10	1.11	1.06
no. of used reflns	1880	1859	1541	2427	3260	1824
R	0.083	0.073	0.091	0.087	0.057	0.091
temp./ °C	25	-50	25	-50	-50	-50

2-3 Results and Discussion

Structure of 1-Alkylthymine Crystals Obtained from *DMF*

Six single crystals of 1-alkylthymine were obtained from DMF for 1-octylthymine (**C8**), 1-undecylthymine (**C11**), 1-dodecylthymine (**C12**), 1-tridecylthymine (**C13**), 1-tetradecylthymine (**C14**), and 1-hexadecylthymine (**C16**); the crystal data for these crystals are tabulated in Table 2. The single crystals for the longer alkyl chain (**C14** and **C16**) were obtained from benzene as well as DMF. Unfortunately, single crystals suitable for X-ray crystal analysis were not obtained for 1-nonylthymine (**C9**), 1-decylthymine (**C10**), and 1-pentadecylthymine (**C15**).

The crystal data in Table 2 show the dependence on the chain length of the alkyl chains for the plates obtained from DMF. When the carbon number of the alkyl chain is odd, the values of ***c*** axis is shorter, and the ***β*** value is smaller than the values for the compounds hav-

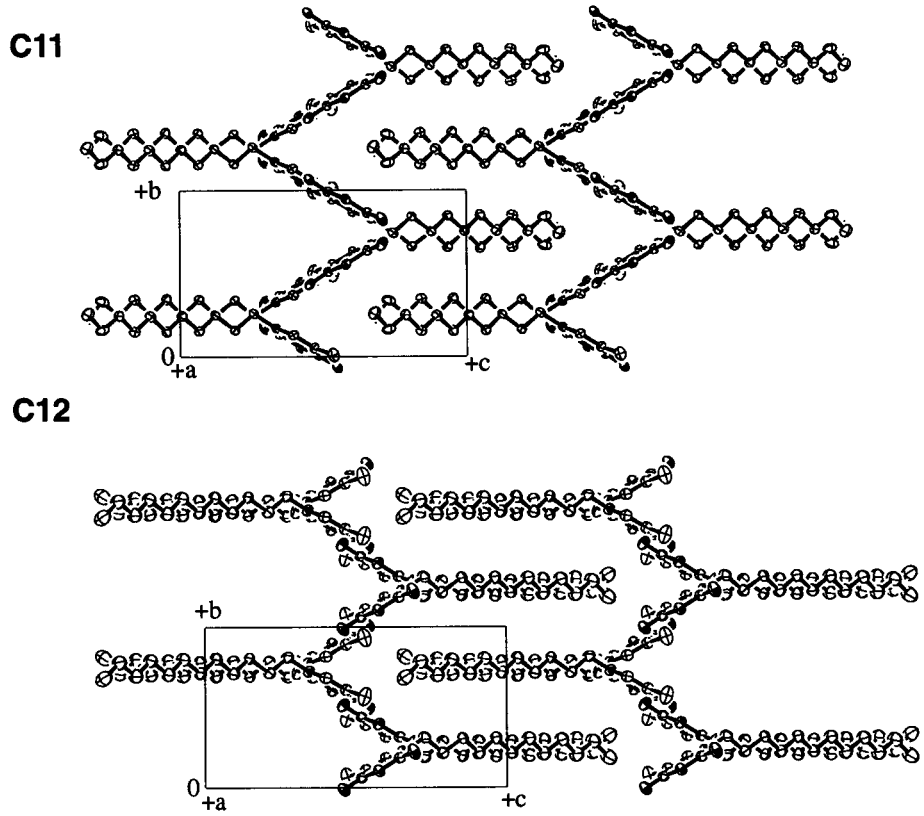

Fig. 3 Molecular packing of 1-undecylthymine (**C11**) and 1-dodecylthymine (**C12**) along ***a*** axis.

ing even numbered carbon atoms of the alkyl chain.

Molecular packing along ***a*** axis is shown in Fig. 3 for **C11** and **C12**. In this figure, the structure of **C11** having odd-numbered alkyl chain is similar to the structure of **C12** having even-numbered alkyl chain. Molecular packing along ***b*** axis in Fig. 4, however, shows clearly the difference between even-numbered and odd-numbered alkyl chains. The β value of **C11** is nearly a right angle (96.51°), and the β value of **C12** is large (114.28°). The difference of these values reflects the angle between thymine bases and the alkyl chains, which extend along ***ac*** plane.

The nearest neighboring molecules are picked up from the crystal structures in Fig. 4 for **C11** and **C12** to give Fig. 5. The molecular packing of 1-undecylthymine (**C11**) along ***b*** axis (Fig. 4 (**C11**)) showed that the alkyl chains were curved and arranged face to face or back to back. The view of the pairs from ***b*** axis for the face to face pair is shown in a rectangle of Fig. 5 (**C11**). In this figure, the thymine rings of molecules (**d**) and (**c**) are not parallel, the alkyl

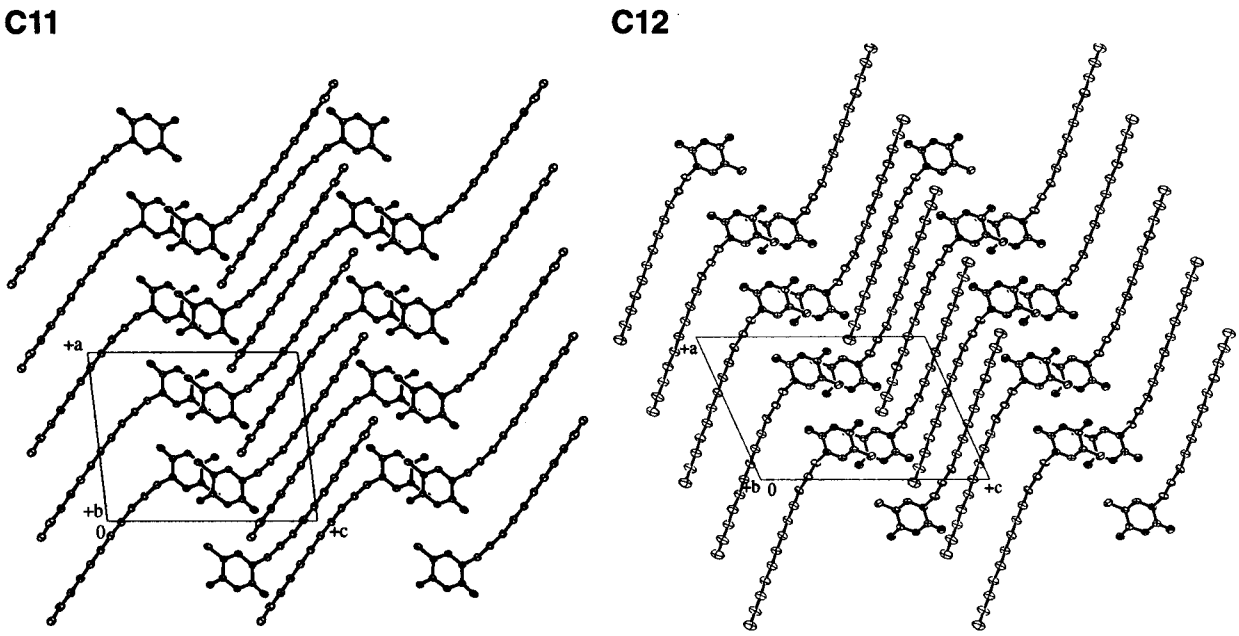

Fig. 4 Molecular packing of 1-undecylthymine (**C11**) and 1-dodecylthymine (**C12**) along ***b*** axis.

chains are face to face, and the terminal methyl group of the molecule (**d**) approaches to the double bond of the thymine base in the molecule (**c**) (3.64 Å). The terminal methyl group of the molecule (**c**), on the other hand, approaches to the thymine base of the molecule (**b**) (3.64 Å). Then the molecules of **C11** connected like a helix. In the case of **C12**, however, the thymine rings arrange parallel for the molecules where the alkyl chains are face to face as shown in a rectangle of Fig. 5 (**C12**). This figure indicates that the terminal methyl group of the molecule (**b**) is closely located to the double bond of the thymine base in the molecule (**a**) with the distance of 3.62 Å, and the terminal methyl group of the molecule (**a**) is closely located to the thymine base of the molecule (**b**). Then two molecules in the crystal of **C12** form a pair instead of a helix.

The carbon number dependence of the crystal structure in Fig. 5 was caused by the direction of the methyl group. The direction of the terminal methyl group in the odd-numbered alkyl chain (**C11**) is opposite to the direction of the thymine bases (**b** and **d** in Fig. 5(**C11**)). Then the methyl group approaches to the upper thymine base (**a** and **c** in Fig.

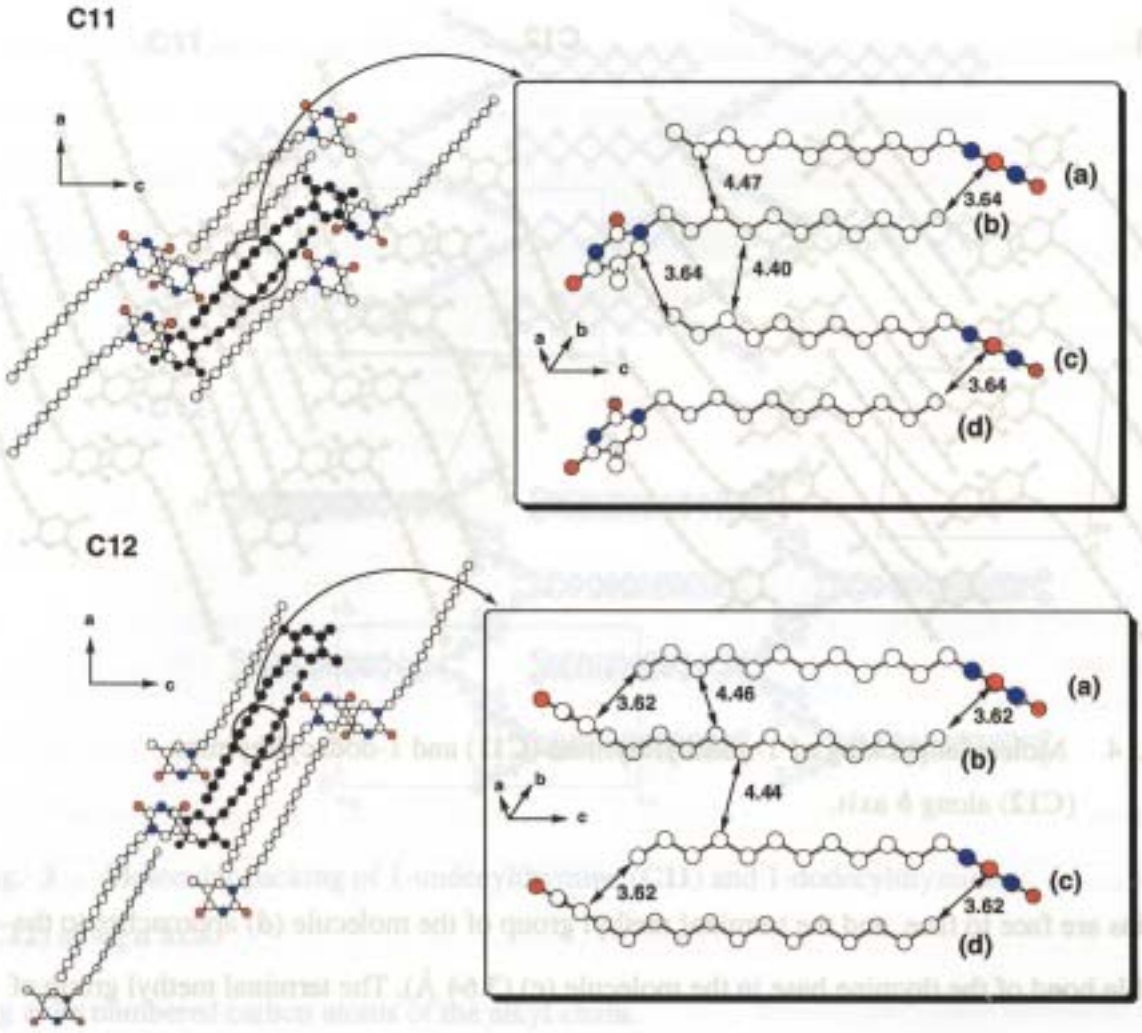

Fig. 5 Neighboring molecules for 1-undecylthymine (**C11**) and 1-dodecylthymine (**C12**).

5(**C11**)). When the carbon number of the alkyl chain is even (**C12**), the direction of the terminal methyl group is the same as the direction of the thymine bases (**b** and **d** in Fig. 5(**C12**)) forming the pairs (**a-b** and **c-d**). The difference of the interaction between the methyl group and the thymine base caused the difference of ***c*** axis and the value of β. The interaction between the terminal methyl group and the thymine base observed in these crystals should be the van der Waals interaction.

Photodimerization of 1-Octylthymine

UV light was irradiated on the single crystal obtained from DMF for 1-octylthymine using an optical fiber with cut-filter (above 280 nm). The photodimerization of the thymine

bases was followed by UV spectra at 270 nm in chloroform solution. Decrease of UV absorption at 270 nm, however, was not detected after irradiation for 2 days. The photodimerization occurred for the crystals of 1-octylthymine in **Form I**[13] and **Form III**[15], while **Form II**[14] was inactive for the photodimerization. Irradiation of UV light on the crystal of **Form I** gave the photodimer quantitatively within 2 h, which was detected by UV, IR, and NMR spectra. The crystal after photodimerization, however, was found to be amorphous from powder X-ray diffraction.[13] The single crystal of **Form III** obtained from acetonitrile also gave the photodimer by irradiation of UV light, although the conversion was lower (60-80% after irradiation for 12 h) than the case of **Form I**.[15] These results indicated that the crystal structure influenced the photoactivity of 1-octylthymine in crystalline state.

Crystal Structure and Photodimerization of 1-Octylthymine

In order to find the relationship between the crystal structure and the photoactivity for the photodimerization, the crystal structures of 1-octylthymine were compared for **Forms I, II, III,** and **IV**. From the crystal structure of 1-octylthymine, we will study the factors determining the activity of the crystals for the photodimerization. The possible factors for the

Table 3 Data of 1-Octylthymine Crystals related to the Photodimerization.

		Form I [13]	Form II [14]	Form III [15]	Form IV
Thymine - Thymine (Å) [(a)]		3.40	4.34	4.47, 4.71	4.36, 4.56
Thymine – Methyl (Å) [(b)]					
[Thymine]	5C	4.26	3.86	7.34	3.64
	6C	4.55	3.86	6.90	3.60
	5Me	5.14	3.96	7.80	3.86
DSC(°C)		108.9,119.9	120.1	59.3, 120.1	122.6

(a)The distance between the adjacent double bonds of thymine bases (Fig. 7).
(b)The distance between the thymine bases and the terminal methyl group of alkyl chain (Fig. 8).

crystal structure are summarized in Table 3.

An important feature of the thymine compounds is the hydrogen bonding between thymine bases. The hydrogen bondings of the thymine bases do not directly influence the photoactivity, but are important for the stability of the crystal structure. The crystallization of 1-octylthymine from solution may begin from the hydrogen bonding of the thymine bases, followed by aggregation of the long alkyl chains. Figure 6 shows the hydrogen-bonded pairs for four crystal forms of 1-octylthymine. In **Form I** and Form **II**, the long alkyl chains extended to the same direction from the plane of the hydrogen bonded thymine bases. On the other hand, in the case of **Form III** and **Form IV**, the long alkyl chains extended in the opposite direction from the plane of the hydrogen bonded thymine bases. The direction of the long alkyl chain may determine the aggregation of the long alkyl chains and the crystal structure. The interaction of the solvent with the molecules may cause the direction of the long alkyl chain during crystallization in solution.

An important factor of the crystal structure for the photoactivity is the distance between the C5-C6 double bonds of the thymine bases, as proposed by Schmidt and his coworkers.[16] Two facing thymine bases in crystals are shown in Fig. 7 for four crystal forms of 1-octylthymine, and the distances between the adjacent double bonds of thymine bases are tabulated in Table 3. The distances between the thymine bases in **Form IV** are 4.36 Å and

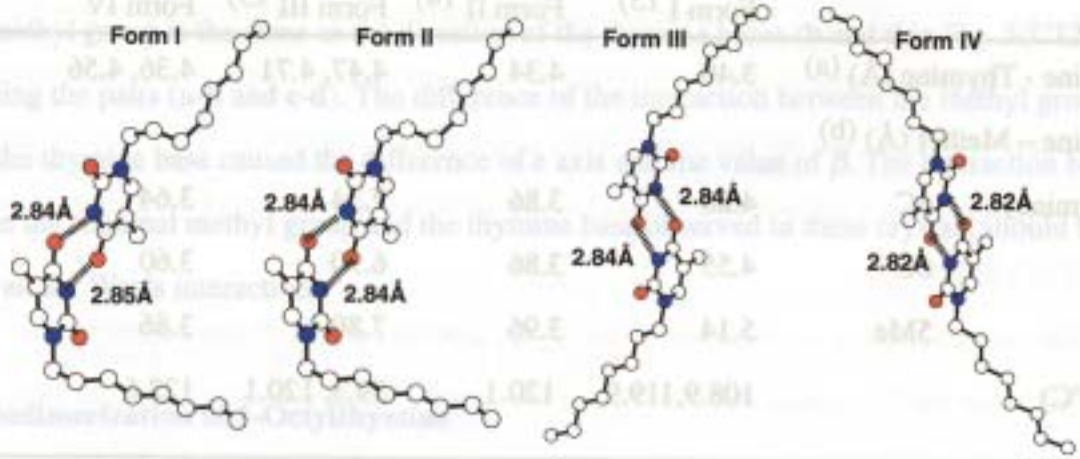

Fig. 6 Hydrogen bonded pairs of 1-octylthymine for **Form I**, **Form II**, **Form III**, and **Form IV**.

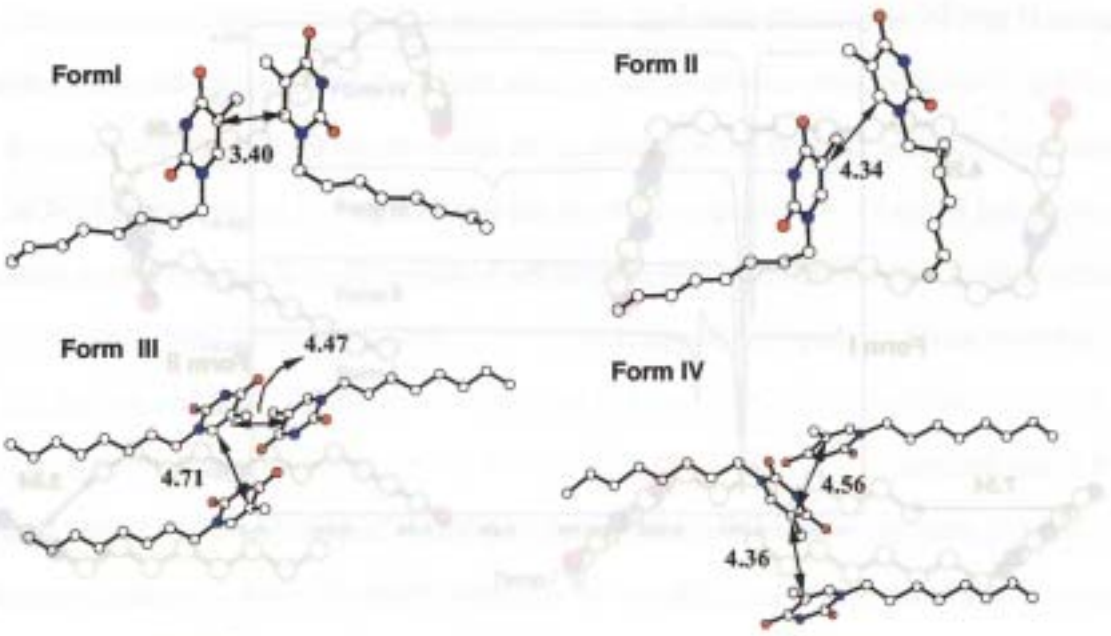

Fig. 7 Facing thymine bases in **Form I**, **Form II**, **Form III**, and **Form IV**.

4.56 Å, which are longer than the distance of the photoactive **Form I** (3.40 Å)but shorter than the distance of the photoactive **Form III** (4.47 and 4.71 Å). Therefore, the distance between the double bonds of the thymine bases is not the main factor for the photodimerization of thymine bases in crystal.

As mentioned above, the characteristic of the crystal structure for **Form IV** is the presence of the terminal methyl group in the vicinity of the double bond in thymine base. The nearest neighboring terminal methyl groups and thymine bases are picked out from the crystal structure of 1-octylthymine for **Forms I, II, III** and **IV** in Fig. 8, and the distances are tabulated in Table 3. The distance between the methyl group and the thymine base (C5) are long for the photoactive **Form I** (4.26 Å) and **Form III** (7.34 Å), but are short for the inactive **Form II** (3.86 Å) and **Form IV** (3.64 Å). The terminal methyl group of the alkyl chain should be important for the photodimerization of the thymine bases, although the methyl group did not participate directly in the photodimerization.

The DSC curves of 1-octylthymine indicate the stability of the crystals (Fig. 9). The inactive crystals of **Form II** and **Form IV** gave only one peak at high temperature around 120

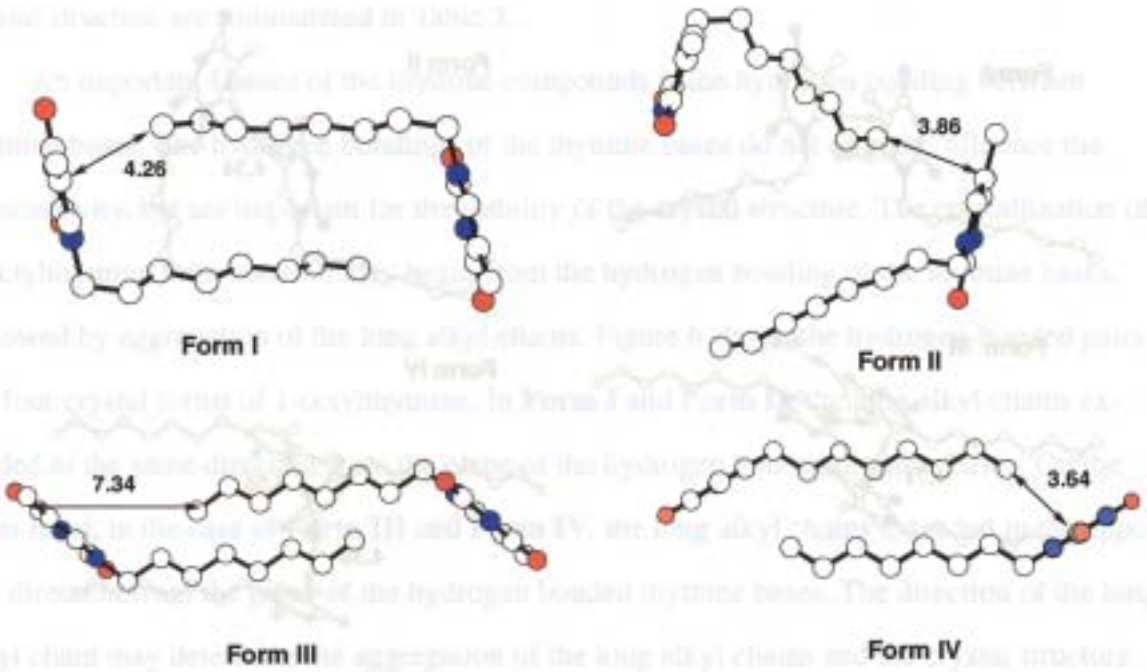

Fig. 8 The nearest neighboring molecules of 1-octylthymine for **Form I**, **Form II**, **Form III**, and **Form IV**.

°C. The photoactive crystals of **Form I** and **Form III**, however, had one more peak in DSC. **Form III** including acetonitrile molecules released acetonitrile at 59.3 °C, followed by melting at 120.1 °C. **Form III** underwent photodimerization, but became inactive after annealing at 100 °C.[15] **Form I** was also active for the photodimerization, but became inactive after annealing at 100 °C.[13] Then, the unstable crystals suggested by the DSC curves were active for the photodimerization.

The alignment of the active double bonds is one more important factor for the photodimerization, as proposed by Schmidt and his coworkers.[16] From the molecular arrangement of the thymine bases in crystal and the structure of the photodimer, the thymine bases were concluded to rotate in opposite directions (disrotation) in the crystal during photodimerization reaction.[13] Conrotatory motion and disrotatory motion were proposed for thermal and photo cyclization of polyene compounds by Woodward and Hoffmann.[17] The photodimerization of the thymine bases is an intermolecular reaction, but the interaction of the alkyl chain may make the photodimerization in crystal to become an intramolecular reac-

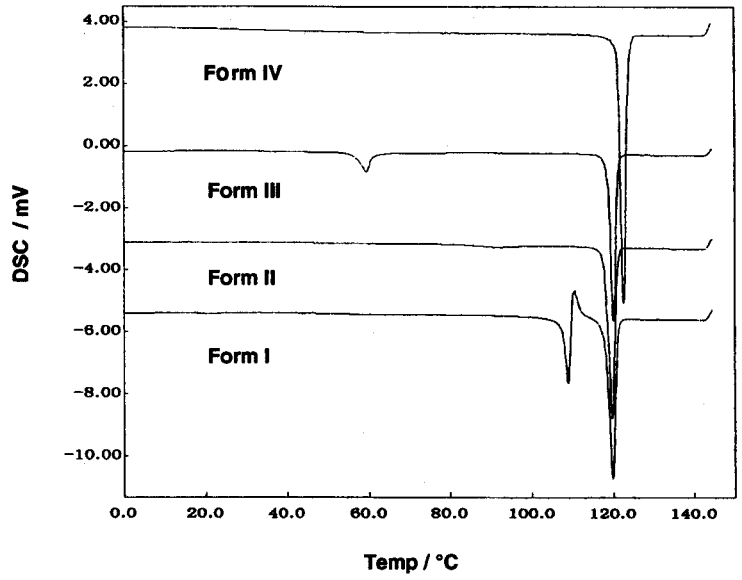

Fig. 9 DSC of 1-octylthymine for **Form I**, **Form II**, **Form III**, and **Form IV**.

tion. Therefore, the alignment of the thymine bases in crystal is not the important factor for the photodimerization, but determines the structure of the photodimer after the disrotatory motion during the photodimerization reaction.

In photoactive **Form I**, the distance between the double bonds of the thymine bases is short (3.40 Å), and the terminal methyl group of the alkyl chain is not near the thymine base (4.26 Å). The DSC data of **Form I** indicate that the crystal is unstable to change to the stable crystal. Consequently, the thymine bases in **Form I** can rotate in crystal to give the photodimer. In photoactive **Form III** from acetonitrile, the distance between the photoactive double bonds of the thymine base was 4.36 Å, which was longer than 4.2 Å of Schmidt's rule. However, the distance between the methyl group and the thymine base (C5) are long enough (7.34 Å) for the disrotatory motion of the thymine bases in crystal. The DSC data also support the instability of the crystal in **Form III**. Therefore, the crystal of **Form III** is active for photodimerization to give the photodimer.

When the terminal methyl group of the long alkyl chain is closely located to the double bond of thymine bases, the terminal methyl group of the alkyl chain should block the rotation of the thymine bases during photodimerization. The DSC data indicated that the crystals of

Forms II and **IV** were stable and could not transform to another crystal form. Therefore, the blocking of the disrotatory motion of the thymine base by the terminal methyl group of the alkyl chain was concluded to be the reason of the inactivity for the photodimerization of **Form II** and **Form IV**. The distance between the terminal methyl group and the C5-C6 double bond of thymine bases is a measure of the blocking effect of the disrotatory motion of the thymine base by the methyl group.

2-4 Conclusion

Single crystals of 1-alkylthymine having long alkyl chain were obtained from *N, N*-dimethylformamide solution, and the crystal structure (**Form IV**) was determined by X-ray crystal analysis. The most remarkable feature of the crystal structure for **Form IV** was the short distance between the terminal methyl group of the long alkyl chain and the double bond of the thymine bases. For 1-alkylthymine having even-numbered alkyl chain, two molecules formed a pair by the interaction of alkyl chains and the interaction of the terminal methyl group with the thymine bases. For 1-alkylthymine having odd-numbered alkyl chain, on the other hand, molecules connected like a helix.

Irradiation of UV light on the crystal of 1-alkylthymine obtained from DMF did not give the photodimer. Factors of the crystal structure affecting the photoactivity of 1-alkylthymine were determined by comparing the crystal structures of 1-octylthymine for **Forms I, II, III,** and **IV**. The distance between the active double bonds of thymine bases could not explain the photoinactivity of 1-octylthymine crystals. The photoinactivity was found to relate closely to the distance between the terminal methyl group of alkyl chain and the double bond of the thymine base. The disrotatory motion of the thymine base is necessary for the photodimerization of 1-octylthymine in crystal, but the closely situated terminal methyl group inhibits the rotation of the thymine base. Therefore, it is concluded that the important factor of the crystal structure for inactivity of the photodimerization of the thymine base is the inhibition of the disrotatory motion by the terminal methyl group of the alkyl chain.

We are grateful to Prof. T. Kitayama , Dr.K.Ute and Mr.T.Kawauchi for DSC measurements.

2-5. References

1. G. J. Fisher and H. E. Johns, "Photochemistry and Photobiology of Nucleic Acids," ed by S. Y. Wang, Academic Press, New York (1976), Vol. I, pp. 225-294.

2. M. H. Patrick and R. O. Rahn, "Photochemistry and Photobiology of Nucleic Acids," ed by S. Y. Wang, Academic Press, New York (1976), Vol. II, pp. 35-95.

3. Y. Inaki, M. J. Moghaddam, and K. Takemoto, "Polymers in Microlithography Materials and Process," ed by E. Reichmanis, S. A. MacDonald, and T. Iwayanagi, American Chemical Society, Washington (1989), ACS Sym. Ser., 412, pp. 303-318.

4. Y. Inaki, N. Matsumura, K. Kanbara, and K. Takemoto, "Polymers for Microelectronics, " ed by Y. Tabata, I. Mita, S. Nonogaki, K. Horie, and S. Tagawa, Kodansha-VCH, Tokyo (1990), pp. 91-102.

5. Y. Inaki, N. Matsumura, and K. Takemoto, "Polymers for Microelectronics," ed by L. F. Thompson, G. Willson, and S. Tagawa, American Chemical Society, Washington (1994), ACS Sym. Ser., 537, pp. 142-164.

6. Y. Inaki, *Polymer News,* **17**, 367-371 (1992).

7. Y. Inaki, "Progress Polymer Science," ed by O. Vogl, Pergamon Press, Oxford (1992), Vol. 17, pp. 515-570.

8. T. Sugiki, N. Tohnai, E. Mochizuki, T. Wada, and Y. Inaki, *Bull. Chem. Soc. Jap.*, **69**, 1777 (1996).

9. N. Tohnai, M. Miyata, and Y. Inaki, *J. Photopolym. Sci. Technol.*, **9**, 63 (1996).

10. N. Tohnai, T. Sugiki, E. Mochizuki, T. Wada, and Y. Inaki, *J. Photopolym. Sci. Technol.*, **7**, 91 (1994).

11. Y. Inaki, Y. Wang, M. Kubo, and K. Takemoto, *J. Photopolym. Sci. Technol.*, **4**, 259-266 (1991).

12. Y. Inaki, Y. Wang, T. Saito, and K. Takemoto, *J. Photopolym. Sci. Technol.*, **5**, 567-568

(1992).

13. N. Tohnai, Y. Inaki, M. Miyata, N. Yasui, E. Mochizuki, and Y. Kai, *J. Photopolym. Sci. Technol.*, **11**, 59 (1998).

14. N. Tohnai, Y. Inaki, M. Miyata, N. Yasui, E. Mochizuki, and Y. Kai, *Bull. Chem. Soc. Jpn.*, **72**, 851-858 (1999).

15. N. Tohnai, Y. Inaki, M. Miyata, N. Yasui, E. Mochizuki, and Y. Kai, *Bull. Chem. Soc. Jpn.*, **72**, 1143-1151 (1999).

16. M. D. Cohen and G. M. J. Schmidt, *J. Chem. Soc.*, 1996 (1964).

17. R. B. Woodward and R. Hoffmann, *J. Am. Chem. Soc.*, **87**, 395 (1945).

Crystal Structure and Photodimerization of 1-Alkylthymine: Effect of Long Alkyl Chain on Isomer Ratio of Photodimer

3-1 Introduction

Thymine derivatives give photodimers under irradiation of UV light at 280 nm.[1)] Photodimeriztion of thymine derivatives is reversible to give original thymine derivatives under UV irradiation at 240 nm (Fig. 1). The reversible photodimerizations are applicable to photoresists and reversible photorecord-ing materials.[2, 3)] Crystal structure and photodi-merizations have been studied for 1-alkylthymine derivatives to clear mechanism of photodimerization in solid state.[4-11)] Polymorphism was found in crystals of 1-alkylthymines. Crystal structure was found to affect on photodimerization of thymine bases in crystals. Single crystals of 1-octylthymine obtained from ethyl acetate[9)] gave photodimer, but crystals obtained from ethanol[10)] did not give photodimers.

Polymorphism of 1-alkylthymine is related to length of alkyl chains and solvent used for crystalliz-ation. Crystal structure of 1-octylthymine (**C8**) obtained from ethyl acetate solution is shown in Fig. 2 (**Type 1**), where hydrogen-bonded thymine bases form plates and alkyl chains

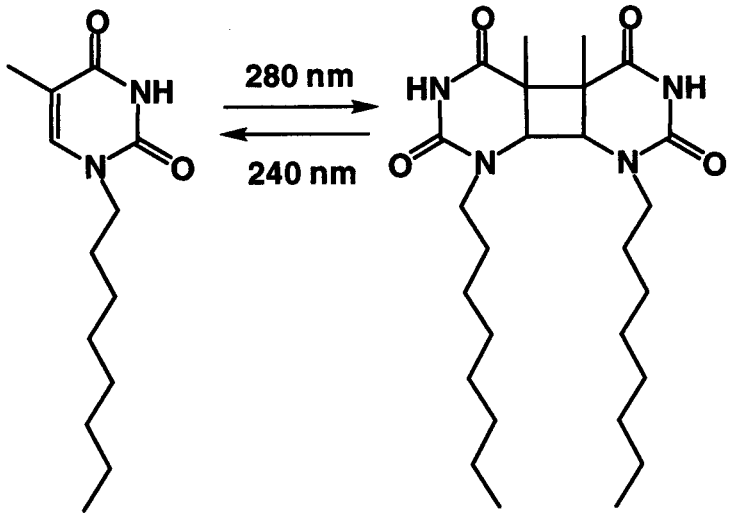

Fig. 1 Photodimerization of 1-alkylthymine.

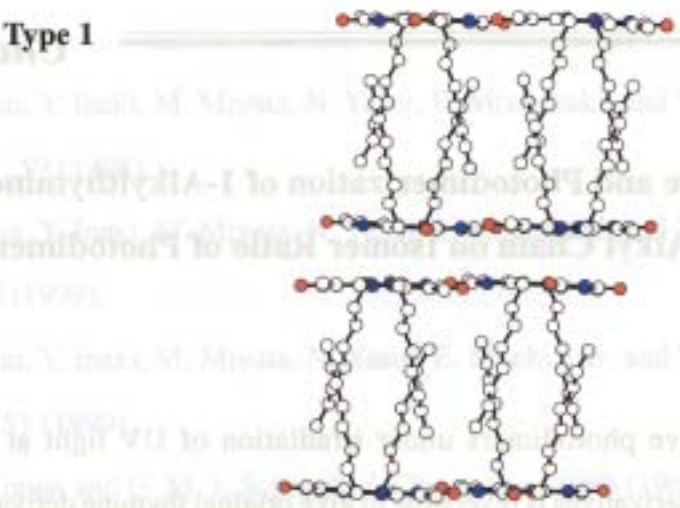

Fig. 2 Molecular packing of 1-octylthymine (**C8**) crystals obtained from ethyl acetate solution.[9)]

form aggregates.[9)] In **Type 1** crystals, thymine bases stacked each other between two plates.

Crystal structure of 1-undecylthymine (**C11**) obtained from *N, N*-dimethylformamide solution is shown in Fig. 3 (**Type 2**), where alkyl chains aggregate regularly but thymine bases do not stack.[12)] Crystals of **Type 1** are photoactive to give photodimers in crystals under irradiation of UV light at 280 nm. **Type 2** crystals, however, hardly give photodimers. This paper deals with **Type 1** crystals and effects of length of alkyl chains on crystal structure and photodimerization. **Type 1** crystals of 1-pentylthymi-ne (**C5**), 1-nonylthymine (**C9**), and 1-decylthymine (**C10**) gave photodimers. The isomers of photodimer obtained from these crystals were different from

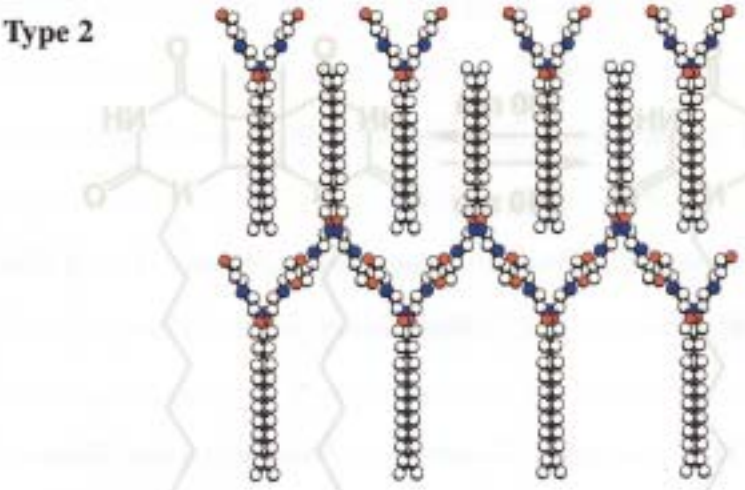

Fig. 3 Molecular packing of 1-undecylthymine (**C11**) crystals obtained from *N, N*-dimethylformamide solution.[12)]

the isomer obtained from 1-octylthymine (**C8**). Different crystal structure was related to different mechanism of photodimerization.

3-2 Experimentals

Materials

Preparations of the 1-alkylthymines are reported in our previous papers.[9, 10, 11] Solvents used for recrystallization were purified by a conventional method.

Instruments

Photodimerizations of the thymine bases in the single crystals (crystal size was around 0.5 x 0.2 x 0.05 mm) were carried out by SUPER CURE-203S UV, where the light source was a Hg-Xe lamp (200 W) (San-Ei Electric) with a cut filter (Toshiba U340).[9] The photodimerization was followed by measuring UV spectra (Nihon Bunko UV/VIS 600) in chloroform solution.

Crystal Structure Analysis

Data of X-ray diffraction for 1-alkylthymine were collected by a Rigaku RAXIS-CS imaging plate two-dimensional area detector using graphite-mono-chromatized Mo-*Ka* radiation (l= 0.71070Å). Using TEXSAN software package of the Molecular Structure Corporation we performed all the crystallographic calculations. The crystal structures were solved by the direct

Table 1 Crystal Data of 1-Alkylthymine.

Compound	**C5**	**C8-1**[a]	**C8-2**[b]	**C9**	**C10**
Crystal system	monoclinic	monoclinic	monoclinic	monoclinic	monoclinic
Space group	$P2_1/c$	$C2/c$	$P2_1/c$	$P2_1/c$	$P2_1/c$
a / Å	11.201(3)	32.34(1)	15.11(1)	16.247(5)	16.161(4)
b / Å	11.700(7)	11.790(6)	12.115(4)	11.758(7)	11.786(5)
c / Å	17.062(5)	17.538(8)	16.471(5)	17.442(4)	17.685(3)
β / °	104.34(3)	112.65(2)	106.35(5)	116.99(3)	103.29(2)
V / Å^3	2234(1)	6171(5)	2894(2)	2969(2)	3278(1)
Z	8	16	8	8	8
D_{calc}	1.166	1.026	1.104	1.129	1.079
R factor	0.089	0.116	0.083	0.092	0.128
Temp. / °C	-50	-50	room	-50	-50

a) Obtained from ethyl acetate solution.[9] b) Obtained from ethanol solution.[10]

methods (shelxs97) and refined by the full-matrix least squares. The positions of hydrogen atoms attached to nitrogen atoms were obtained from the difference Fourier syntheses. All non-hydrogen atoms and hydrogen atoms were refined anisotropically and isotropically, respectively. The crystal data of six thymine derivatives are shown in Tab. 1.

3-3 Results and Discussion

Photodimerization of 1-Alkylthymines

Photodimerizations of 1-alkylthymine in solution gave four isomers of photodimers (Fig. 4 and Tab. 2).[9] **Type 1** crystals of 1-octylthymine (**C8**) gave only *trans-anti* isomers. In the case of 1-pentyltymine (**C5**) and 1-nonylthymine (**C9**) gave *trans-syn* isomers of photodimers. **Type 1** crystals of 1-undecylthymine (**C10**) gave mixture of isomers, *trans-anti* and *trans-syn*. Conversion of photodi-merization for **C8** was high (98 %) but conversions of **C5**, **C9**, and **C10** were low around 30 %.

Crystal Structure

Type 1 crystals were obtained for 1-alkylthymine with short alkyl chains such as **C5**. With increase of chain length, both **Type 1** and **Type 2** crystals were obtained from **C8** to **C10**. For **C9** and **C10**, **Type 2** crystal was too unstable to isolate, but DSC data indicated the presence two

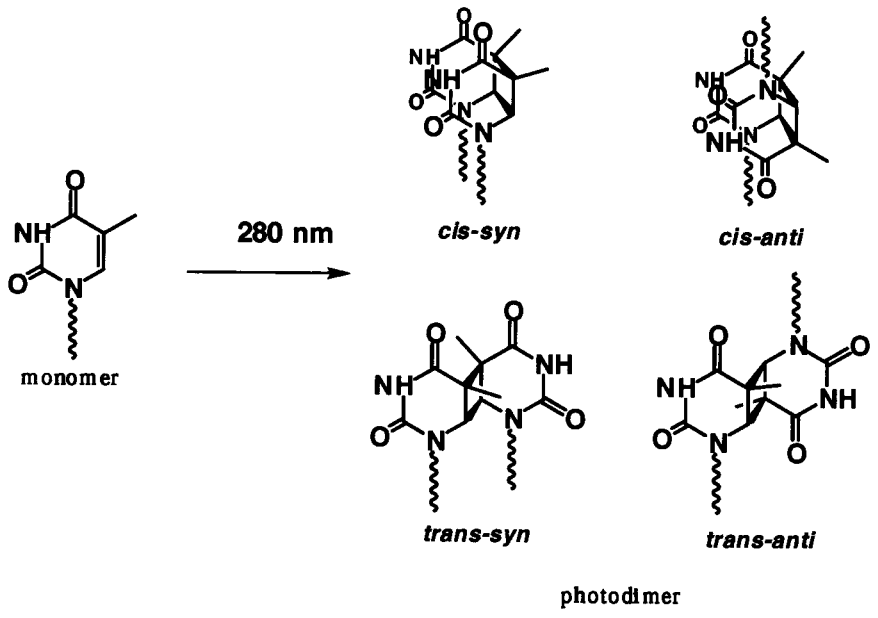

Fig. 4 Four isomers of thymine photodimers.

Tab. 2. Conversion and isomer ratios of photodimerization in single crystals.

Compound	Solution[9)]	Pentyl(**C5**)	Octyl(**C8**)	Nonyl(**C9**)	Decyl(**C10**)
conversion	-	30 %	98 %	30 %	40 %
cis-syn	0.85	-	-	-	-
cis-anti	0.76	-	-	-	-
trans-syn	1.00	1.0	-	1.0	0.7
trans-anti	0.95	-	1.0	-	0.3

crystal forms. For 1-alkylthymine with long alkyl chains above **C11**, only **Type 2** crystals were obtained. Crystallization of 1-alkylthymine is competitive crystallization of thymine bases with alkyl chains (Fig. 5). For compounds with short alkyl chains, thymine bases crystallized in preference to alkyl chains to form **Type 1** crystals. For compounds with long alkyl chains, alkyl chains crystallized in preference to thymine bases to form **Type 2** crystals.

Crystal structures of **Type 1** for **C5**, **C9** and **C10** are shown in Fig. 6 with the data of **C8**. In **Type 1** crystals, the hydrogen-bonded thymines form a plate by dipole interaction, and form parallel plates by stacking interaction. The bilayer of thymine bases piles up by aggregation of alkyl chains. Style of aggregation of alkyl chains depends on length of alkyl chains (circle in Fig. 6).

Fig. 7 shows pairs of hydrogen-bonded thymine bases for **C5**, where one of the hydrogen-bonded thymine base stacked with one thymine of the another pair. In the same plane, thymine base interacts by dipole interaction forming a plate (Fig. 8). Hydrogen bonding and conformation of faced thymines were the same for **C5**, **C9**, and **C10**, while style of aggregation of alkyl

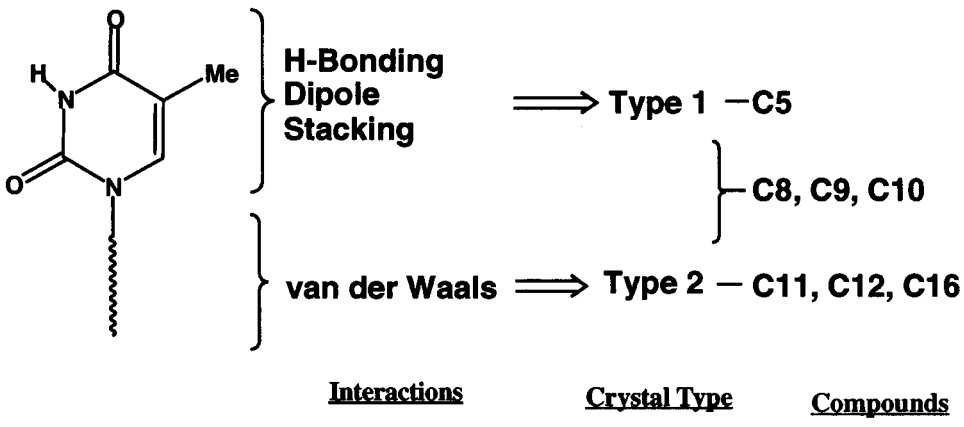

Fig. 5 Interactions and crystallization of 1-alkylthymine.

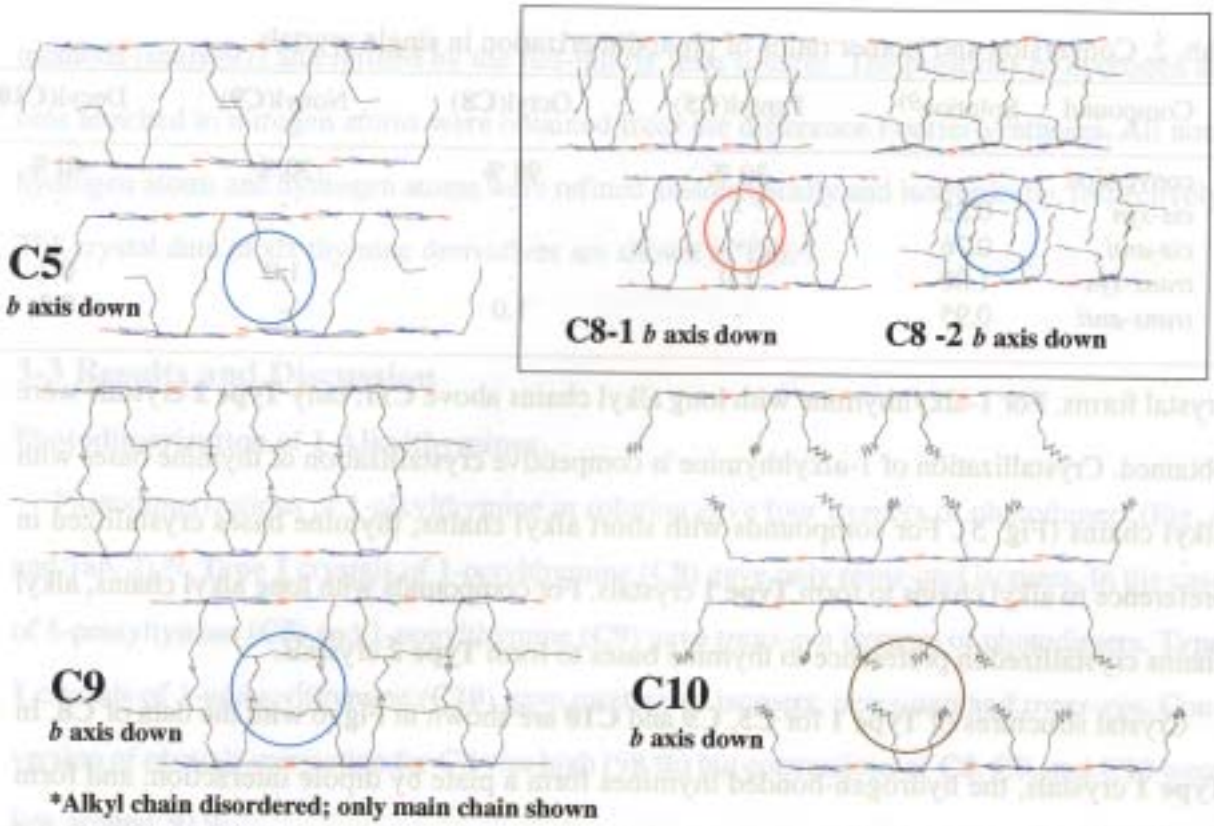

Fig. 6 Molecular packing of **Type 1** crystals for **C5**, **C8-1**, **C8-2**, **C9**, and **C10**.

chains was different.

Fig. 6 suggests no significant interaction of alkyl chains for **C10** between two plates of thymine bases. This fact indicates that hydrogen-bonded pair of thymines was first formed during crystallization from solution, followed by formation of two plates by dipole and stacking interactions (**Type 1** in Fig. 9). At last crystals were formed by van der Waals interaction of alkyl

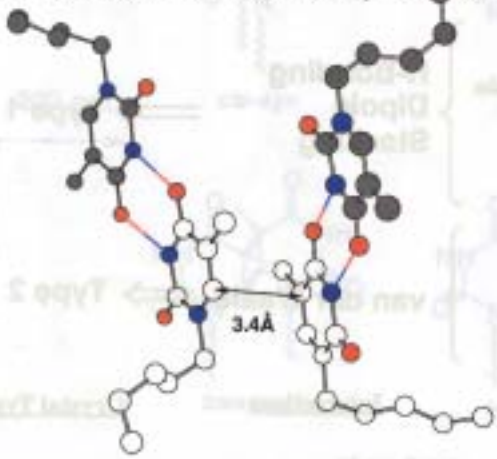

Fig. 7 Hydrogen-bonded thymine pairs of 1-pentylthymine (**C5**).

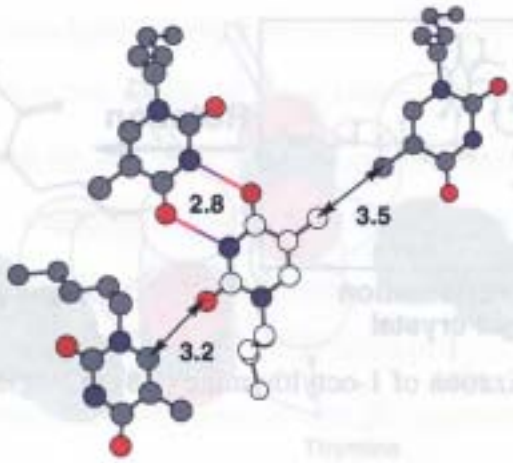

Fig. 8 Hydrogen bonding and dipole interaction of 1-pentylthymine (**C5**) in the same plate.

chains between two plates. When alkyl chains are long, van der Waals interaction of alkyl chains is strong to form regular arrangement of alkyl chains to give **Type 2** crystals.

Conformation of thymines faced each other for photodimerization is *trans-syn* that is the same for **C5**, **C8**, **C9**, and **C10**. Conformation of thymines, therefore, can not explain the difference of photo-dimer isomers. A key factor determines isomers of photodimer should be alkyl chains.

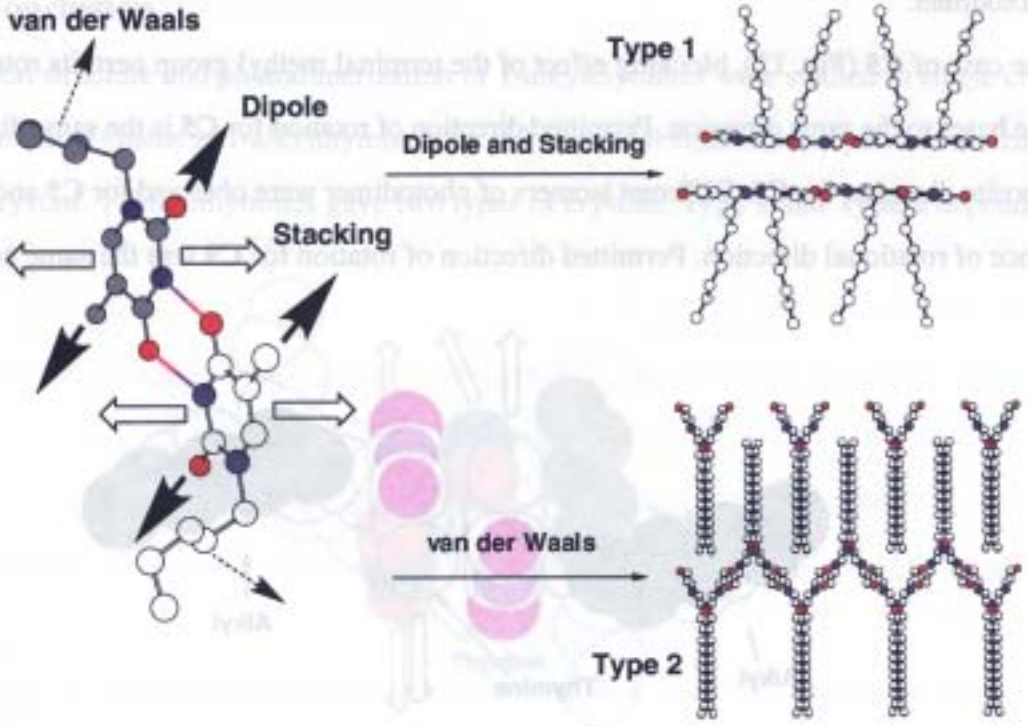

Fig. 9 Interactions and crystallizations of 1-alkylthymine.

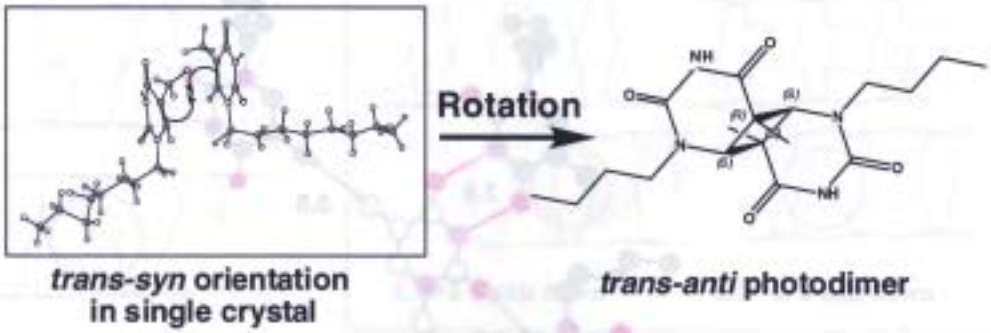

Fig. 10 Photodimerization of 1-octylthymine (**C8**) in single crystals obtained from ethyl acetate solution.[9)]

Active thymine bases for photodimerization are picked up for **C8** to give Fig. 10. Conformation of thymine bases in crystal was *trans-syn*, but the photodimer was *trans-anti*. It was concluded that thymine bases rotated during photodimerization to give *trans-anti* photodimer.[9)]

Fig. 11 shows active thymine bases and surrounding alkyl groups in space filling model for **C8**. In this model, terminal methyl group of alkyl chain is closely located to thymine base. Distance of the methyl group to N3 of thymine was 3.6 Å, and to C5 was 4.3 Å. The methyl groups inhibit rotation of thymine base, and permit opposite directions for two thymine bases as shown in Fig. 11. Permitted rotations of thymine bases during photodimerization may give *trans-anti* photodimer.

In the case of **C5** (Fig. 12), blocking effect of the terminal methyl group permits rotation of thymine bases to the same direction. Permitted direction of rotation for **C5** is the same direction, but opposite direction for **C8**. Different isomers of photodimer were obtained for **C5** and **C8** by difference of rotational direction. Permitted direction of rotation for **C9** was the same as **C5**.

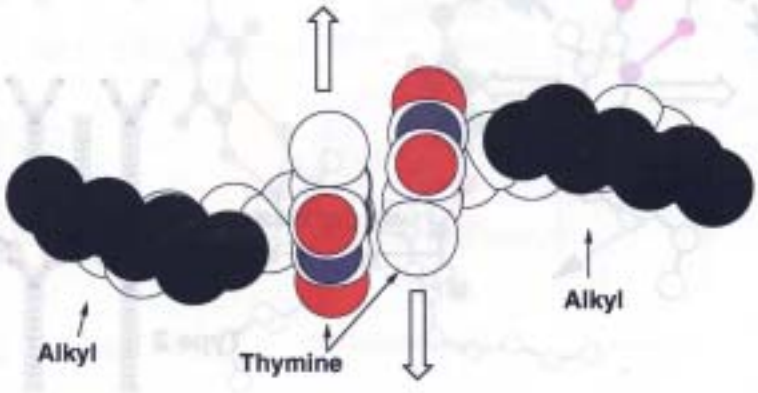

Fig. 11 Restriction of rotation by terminal methyl groups for 1-octylthymine (**C8**).

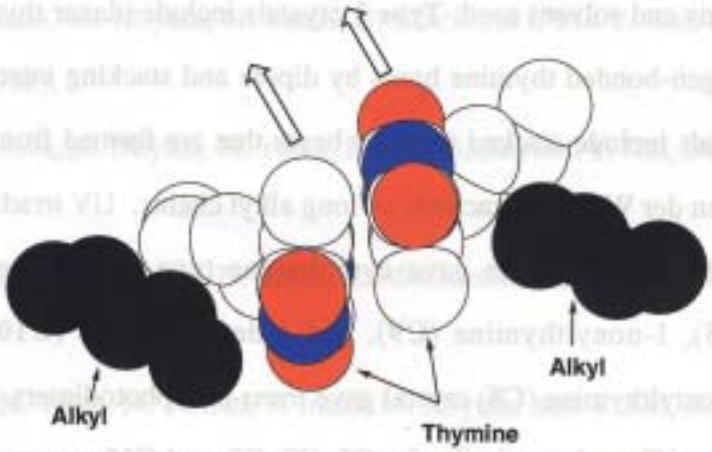

Fig. 12 Restriction of rotation by terminal methyl groups for 1-pentylthymine (**C5**).

In the case of **C10**, alkyl chains of another layer are in a long distance. There are no alkyl chains near thymine base on the left, and rotation of thymine base should be free (Fig. 13). However, rotation of thymine base on the right is inhibited by terminal methyl group of alkyl chain that is in the same plane. Permitted rotation of thymine on the right is only upper direction. Then, two isomers of photodimers, *trans-syn* and *trans-anti* can be obtained for **C10** (Tab. 2).

3-4 Conclusion

Crystal structure and photodimerization of 1-alkylthymines were studied in single crystals. Length of alkyl chains in 1-alkylthymine affected on crystal structure and photodimerization in single crystasl. 1-Alkylthymines gave two types of crystals, **Type 1** and **Type 2** depending on

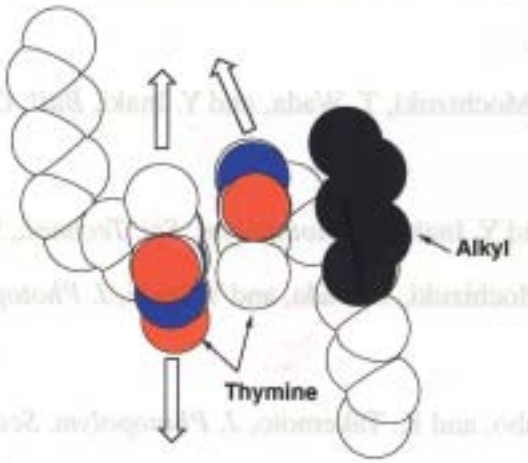

Fig. 13 Restriction of rotation by terminal methyl group for 1-decylthymine (**C10**).

length of alkyl chains and solvent used. **Type 1** crystals include planar thymine bases that are formed from hydrogen-bonded thymine bases by dipole and stacking interactions of thymine bases. **Type 2** crystals include stacked thymine bases that are formed from hydrogen-bonded thymine bases by van der Waals interactions of long alkyl chains. UV irradiation at 280 nm on **Type 1** crystals of 1-alkylthymine gave cyclobutane type photodimers. Crystals of 1-pentylthymine (**C5**), 1-nonylthymine (**C9**), and 1-decylthymine (**C10**) gave *trans-syn* photodimers, but 1-octylthymine (**C8**) crystal gave *trans-anti* photodimers.

Crystal structures of **Type 1** are similar for **C5**, **C8**, **C9**, and **C10**, except interaction of alkyl chains. Alkyl chains played an important role in forming different isomers of photodimers. Terminal methyl groups of alkyl chains locate closely to thymine bases, and inhibit rotation of thymine bases during photodimerization in crystals.

3-5 References

1. G. J. Fisher and H. E. Johns, "Photochemistry and Photobiology of Nucleic Acids," ed by S. Y. Wang, Academic Press, New York (1976), Vol. I, pp. 225-294.

2. Y. Inaki, M. J. Moghaddam, and K. Takemoto, "Polymers in Microlithography Materials and Process," ed by E. Reichmanis, S. A. MacDonald, and T. Iwayanagi, American Chemical Society, Washington (1989), ACS Sym. Ser., 412, pp. 303-318.

3. Y. Inaki, N. Matsumura, and K. Takemoto, "Polymers for Microelectronics," ed by L. F. Thompson, G. Willson, and S. Tagawa, American Chemical Society, Washington (1994), ACS Sym. Ser., 537, pp. 142-164.

4. T. Sugiki, N. Tohnai, E. Mochizuki, T. Wada, and Y. Inaki, *Bull. Chem. Soc. Jap.*, **69**, 1777 (1996).

5. N. Tohnai, M. Miyata, and Y. Inaki, *J. Photopolym. Sci. Technol.*, **9,** 63 (1996).

6. N. Tohnai, T. Sugiki, E. Mochizuki, T. Wada, and Y. Inaki, *J. Photopolym. Sci. Technol.*, **7**, 91 (1994).

7. Y. Inaki, Y. Wang, M. Kubo, and K. Takemoto, *J. Photopolym. Sci. Technol.*, **4**, 259 (1991).

8. Y. Inaki, Y. Wang, T. Saito, and K. Takemoto, *J. Photopolym. Sci. Technol.*, **5**, 567 (1992).

9. N. Tohnai, Y. Inaki, M. Miyata, N. Yasui, E. Mochizuki, and Y. Kai, *J. Photopolym. Sci. Technol.*, **11**, 59 (1998).

10. N. Tohnai, Y. Inaki, M. Miyata, N. Yasui, E. Mochizuki, and Y. Kai, *Bull. Chem. Soc. Jpn.*, **72**, 851 (1999).

11. N. Tohnai, Y. Inaki, M. Miyata, N. Yasui, E. Mochizuki, and Y. Kai, *Bull. Chem. Soc. Jpn.*, **72**, 1143 (1999).

12. E. Mochizuki, N. Yasui, N. Tohnai, Y. Inaki, M. Miyata, and Y. Kai, *Bull. Chem. Soc. Jpn.*, **73**,1035 (2000).

Chapter 4

Single-Crystal-to-Single-Crystal Enantioselective [2+2] Photodimerization of Coumarin and Thiocoumarin in the Inclusion Complexes with Chiral Host Compounds

4-1 Introduction

Photodimerizations of coumarin and its derivatives have been studied extensively. However, it is still difficult to control the regio- and stereoselective [2+2]photodimerization of such enone derivatives both in solution and solid state. For example, photoirradiation of coumarin **1a** in the solid state for 48 h gives a mixture of anti-head-to-head dimer **6a**, syn-head-to-head dimer **7a** and syn-head-to-tail dimer **9** in only 20% yield, while photoirradiation of **1a** in water for 22 h affords **7a** in 20% yield.[1] Photodimerization of thiocoumarin **1b** in the solid state gives a complex mixture of four possible dimers **6b~9b**, although (±)-**6b** is obtained when irradiated in CH_2Cl_2 solution.[2] Photoirradiation of both neat and benzene solutions of cyclohex-2-enone **2** gives a mixture of syn-trans-dimer **10** and anti-trans-dimer **11**.[3] Furthermore, the enantiocontrol of the [2+2]photodimerization reactions of coumarin, thiocoumarin and cyclohex-2-enone has not yet been reported.

Recently, we have found that the stereo-, regio-, and enantio-selective photodimerization reactions of **1a**, **1b** and **2** proceed very efficiently in the inclusion complexes with various host compounds (**3~5**). For example, photoirradiation of the 1:1 inclusion complex **12** of (-)-**3a** with **1a** in the solid state gave optically active anti-head-to-head dimer (-)-**6a** in 96% yield.[4] Similar photoirradiation of the 1:2 inclusion complex of (-)-**5a** with **1a** gave syn-head-to-head dimer **7** in 75% yield, while racemic anti-head-to-tail dimer **8a** was obtained in 92% yield by photoirradiation of the 1:2 inclusion complex of meso-**5b** with **1a**.[4] Photoirradiation of **14**, 1:2 inclusion complex of (-)-**5a** with **1b**, and 1:2 inclusion complex of meso-**5b** with **1b** gave optically pure (+)-**6b**, **7b** and (±)-**8b** in 73, 74 and 69% yields, respectively.[5] Further, photoirradiation of the 1:2 inclusion complex of (-)-**4** with **2** in the solid state afforded (-)-**10** of 48% ee in 75%

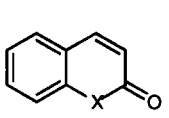

1

a: X=O
b: X=S

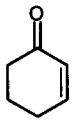

2

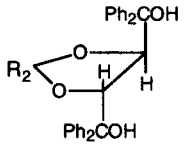

3

a: R_2=Me_2
b: R_2=

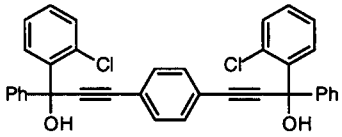

4

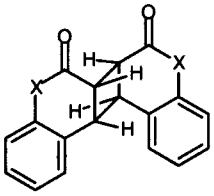

6

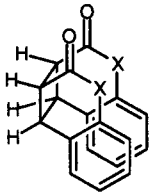

7

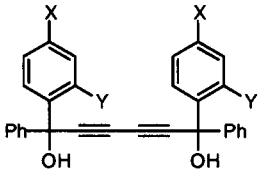

5

a: X=H, Y=Cl
b: X=Y=Me

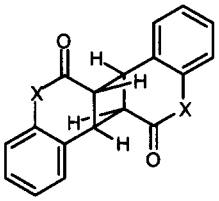

8

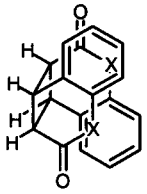

9

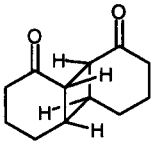

10

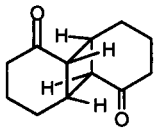

11

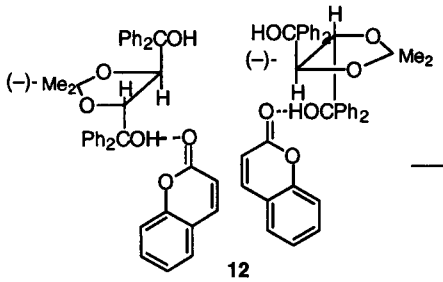

12

hv

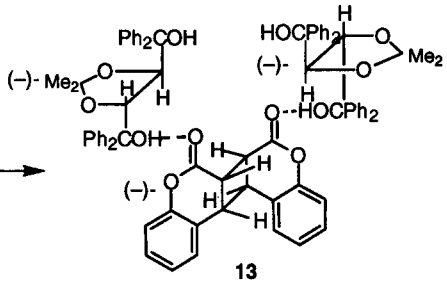

13

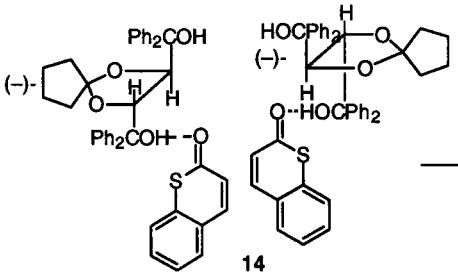

14

hv

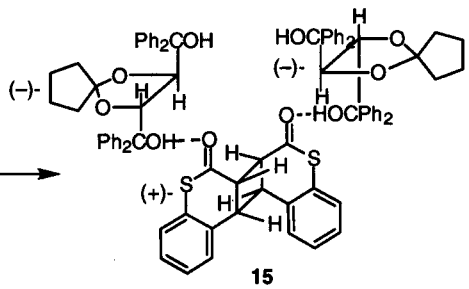

15

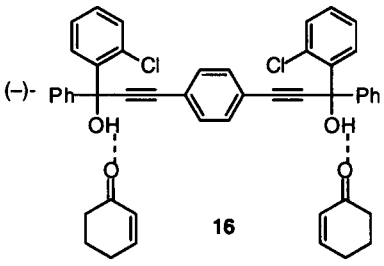

16

hv

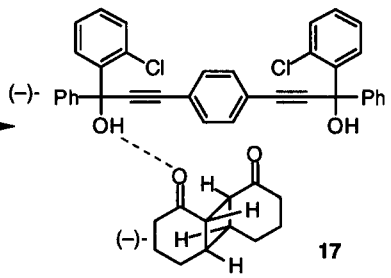

17

yield.[6]

Interestingly, we have now found that the single crystals of the inclusion complexes **12**, **14** and **16** were efficiently converted to the single crystals of the corresponding inclusion complexes **13**, **15** and **17**, respectively, upon photoirradiation in the solid state. Some examples of single-crystal-to-single-crystal photoreaction have been reported previously.[7-11] However, only a few of these involve enantioselective reactions and they are all intramolecular photocyclization reactions.[9-11] This is the first example of enantioselective intermolecular photoreaction via a single-crystal-to-single-crystal transformation in the inclusion complexes with optically active host compounds.

4-2 Experimentals

IR spectra were recorded on a JASCO FT-IR 300 spectrometer, and NMR spectra were measured on a JEOL Lambda-300 spectrometer. Optical rotations were measured on a JASCO DIP-1000 polarimeter.

Photodimerization of coumarin 1a in the inclusion complex 12. When a solution of **1a** (10.0 g, 21.5 mmol) and (-)-**3a** (3.2 g, 21.9 mmol) in AcOEt (20 ml)-hexane (100 ml) was kept at room temperature for 3 h, a 1:1 inclusion complex (**12**) was obtained as colorless needles (5.7 g, 43%, m.p. 95-98 °C).[6] IR (Nujol): nC=O : 1700 cm^{-1}, nC=C : 1607 cm^{-1}, nOH :3358, 3230 cm^{-1}. Elemental analysis calcd. for $C_{40}H_{36}O_6$: C 71.37, H 3.99; found: C 71.64 H 3.82. Photoirradiation of **12** (1.0 g, 1.6 mmol) was carried out in the solid state by using 400 W high-pressure Hg-lamp through Pyrex filter at room temperature for 4 h. This reaction gave a 2:1 complex (**13**) of (-)-**3a** with (–)-**6a**, quantitatively. Colorless needles. M.p. 228-232 °C. IR (Nujol): nC=O: 1740 cm^{-1}, nOH: 3433, 3262 cm^{-1}. Elemental analysis calcd. for $C_{40}H_{36}O_6$: C 71.37, H 3.99; found: C 71.64 H 3.82. When the 2:1 complex (**13**) (1.0 g) was recrystallized from DMF-H_2O (5:1, 5 ml), a 1:1 complex of (-)-**3a** with DMF was obtained as colorless prisms (0.86 g, 99%). Concentration of the filtrate left after separation of the 1:1 DMF complex with (-)-**3a**, optically pure (–)-*anti*-head-to-head dimer (**6a**) (0.17 g, m.p. 168-169 °C, $[a]_D$-9.1 °(*c* 0.19, benzene) , 100% ee) was

obtained as colorless prisms in 89% yield after recrystallization from ethyl acetate-hexane.

Photodimerization of thiocoumarin 1b in the inclusion complex 14. When a solution of **1b** (0.66 g, 4.1 mmol) and (-)-**3b** (2.0 g, 4.1 mmol) in *n*-butyl ether (25 ml)-hexane (5 ml) was kept at room temperature for 12 h, a 1:1 inclusion complex (**14**) was obtained as colorless needles (2.1 g, 76%, m.p. 106-108 °C). IR (Nujol): nC=O : 1618 cm^{-1}, nC=C : 1582 cm^{-1}, nOH : 3358, 3250 cm^{-1}. Elemental analysis calcd. for $C_{42}H_{38}O_5S$: C 77.04, H 5.85; found: C 77.15, H 5.79. Photoirradiation of **14** (1.0 g, 1.5 mmol) was carried out in the solid state by using 400 W high-pressure Hg-lamp through Pyrex filter at room temperature for 2 h. This reaction gave a 2:1 complex (**15**) of (-)-**3b** with (+)-**6b**, quantitatively. Colorless needles. M.p. 190-194 °C. IR (Nujol): nC=O: 1740 cm^{-1}, nOH: 3433, 3262 cm^{-1}. Elemental analysis calcd. for $C_{42}H_{38}O_5S$: C 77.04, H 5.85; found: C 77.12, H 5.90. The 2:1 complex (**15**, 1.0 g) was dissolved in toluene (5 ml) and chromatographed on silica gel using toluene-AcOEt (4:1) to give optically pure (+)-**6b** (0.18 g, 73% yield) as colorless prisms after recrystallization from toluene. M.p. 254-255 °C. $[a]_D$+182 °(*c* 0.02, $CHCl_3$). IR (Nujol): nC=O: 1681, 1655 cm^{-1}. Elemental analysis calcd. for $C_{18}H_{12}O_2S_2$: C 66.64, H 3.73; found: C 66.38, H 3.60.

Photodimerization of cyclohex-2-enone 2 in the inclusion complex 16.

A solution of (-)-**4** (5.0 g, 8.94 mmol) and **2** (1.72 g, 17.9 mmol) in ether-hexane (1:1, 10 ml) was kept at room temperature for 6 h to give a 1:2 complex **16** of (-)-**4** and **2** as colorless prisms (6.1 g, 91% yield). Mp 90-95 °C. IR (Nujol): nC=O: 1660 cm^{-1}. Elemental analysis calcd. for $C_{48}H_{40}O_4Cl_2$: C 76.69, H 5.36; found: C 77.01, H 5.50. Photoirradiation of **16** (2.0 g, 2.66 mmol) in the solid state by using 400 W high-pressure Hg-lamp through Pyrex filter at room temperature for 24 h gave a 1:1 complex (**17**, mp 79-84 °C) of (-)-**4** with (-)-**10**, which upon distillation *in vacuo* gave (-)-**10** of 46 %ee (0.38 g, 75 % yield, $[a]_D$-58.5 °(*c* 0.2, MeOH)). The optical purity was determined by HPLC containing Chiralpak AS (Daicel Chemical Co. Ltd., Himeji, Japan) as the chiral solid phase. Similar photoirradiation of powdered **16** (2.0 g, 2.66 mmol) at –78 °C for 30 h gave (-)-**10** of 58 %ee (0.28 g, 55 % yield, $[a]_D$-73.8 °(*c* 0.25, MeOH)).

Crystal data for a 1:1 complex (12) of 1a with (-)-2a. $C_{40}H_{36}O_6$, FW=612.72 space group monoclinic *C*2, *a*=35.59(4)Å, *b*=9.489(4)Å, *c*=10.03(1)Å, *b*=102.70(4)°, *V*=3305(4)$Å^3$, *Z*=4,

D_{calc}=1.23g/cm^3, crystal dimensions 1.0x0.05x0.03mm, μ=0.82cm^{-1}, T=293K, *R*=0.105, R_w=0.088, and S=2.63 for 561 parameters and 1291 unique observed reflections with [I > 3s(I)], Dr_{max} = 0.37eÅ^{-3}. Data of X-ray diffraction were collected by RIGAKU RAXIS-CS imaging plate two-dimensional area detector with graphite-monochromatized Mo-*K*a radiation (l=0.71070Å) to 2θ max of 59.5°. All the crystallographic calculations were performed by TEXSAN software package of the Molecular Structural Corporation. The crystal structures were solved by the direct methods (LODEM) and refined by the full-matrix least squares. All non-hydrogen atoms and were refined anisotropically and isotropically.

Crystal data for a 2:1 complex (13) of 1a with (-)-3a. $C_{40}H_{36}O_6$, FW=612.72 space group monoclinic *C*2, *a*=32.80(3)Å, *b*=9.467(3)Å, *c*=10.360(4)Å, *b*=100.27(7)°, *V*=3164(2)Å^3, *Z*=4, D_{calc}=1.29g/cm^3, crystal dimensions 0.80x0.05x0.03mm, μ=0.86cm^{-1}, T=293K, *R*=0.114, R_w=0.097, and S=2.86 for 560 parameters and 1939 unique observed reflections with [I > 3s(I)], Dr_{max} = 0.46eÅ^{-3}. Data of X-ray diffraction were collected by RIGAKU RAXIS-CS imaging plate two-dimensional area detector with graphite-monochromatized Mo-*K*a radiation (l=0.71070Å) to 2q max of 59.5°. All the crystallographic calculations were performed by TEXSAN software package of the Molecular Structural Corporation. The crystal structures were solved by the direct methods (LODEM) and refined by the full-matrix least squares. All non-hydrogen atoms and were refined anisotropically and isotropically.

Crystal data for a 1:1 complex (14) of 1b with (+)-2b. $C_{42}H_{38}O_5S_1$, FW=654.82, space group monoclinic $P2_1$, *a*=10.235(2)Å, *b*=35.78(1)Å, *c*=9.422(2)Å, *b*=91.00(2)°, *V*=3449(1)Å^3, *Z*=4, D_{calc}=1.26g/cm^3, crystal dimensions 1.0x0.2x0.15mm, μ=1.36cm^{-1}, T=243K, *R*=0.065, R_w=0.169, and Goodness of Fit(S) =1.07 for 865 parameters and 4954 unique observed reflections with [I > 2s(I)], Dr_{max} = 0.42eÅ^{-3}. Data of X-ray diffraction were collected by RIGAKU RAXIS-CS imaging plate two-dimensional area detector with graphite-monochromatized Mo-*K*a radiation (l=0.71070Å) to 2θ max of 59.9°. All the crystallographic calculations were performed by TEXSAN software package of the Molecular Structural Corporation. The crystal structures were solved by the direct methods (sir92) and refined by shelxl93. All non-hydrogen atoms and were refined anisotropically and isotropically.

Crystal data for a 2:1 complex(15) of 1b with (+)-3b. $C_{42}H_{38}O_5S_1$, FW=654.82, space group monoclinic $P2_1$, a=10.371(3)Å, b=34.70(2)Å, c=9.414(3)Å, b=91.38(2)°, V=3387(2)Å^3, Z=4, D_{calc}=1.28g/cm^3, crystal dimensions 1.0x0.2x0.15mm, μ=1.42cm^{-1}, T=243K, R=0.078, R_w=0.218, and Goodness of Fit(S)=1.01 for 865 parameters and 4104 unique observed reflections with [I > 2s(I)], Dr_{max} = 0.34eÅ^{-3}. Data of X-ray diffraction were collected by RIGAKU RAXIS-CS imaging plate two-dimensional area detector with graphite-monochromatized Mo-*K*a radiation (l=0.71070Å) to 2q max of 59.7°. All the crystallographic calculations were performed by TEXSAN software package of the Molecular Structural Corporation. The crystal structures were solved by the direct methods (LODEM) and refined by shelxl93. All non-hydrogen atoms and were refined anisotropically and isotropically.

Crystal data for 16. $C_{36}H_{24}O_2Cl_2$•$2C_6H_8O$, monoclinic, space group $P2_1$, Mo*K*a radiation, $2q_{max}$=55°, a = 8.411(2), b = 28.774(3), c = 8.696(2) Å, b =105.29(2)°, U =2028.1(8) Å^3. D_c = 1.231 g cm^{-3}, m = 2.03 cm^{-1}, 4775 independent intensities, 4052 observed (I > 1.00s(I)), T = 296K, R = 0.048, R_w = 0.061, GOF = 1.72, maximum residual electron density 0.17eÅ^{-3}.

Crystal data for 17. $C_{36}H_{24}O_2Cl_2$•$2C_6H_8O$, monoclinic, space group $P2_1$, Cu*K*a radiation, a = 8.455(3), b = 28.332(3), c = 8.704(2) Å, b = 106.54(2)°, U = 1998.7(9) Å^3, D_c = 1.249g cm^{-3}, m = 18.06cm^{-1}, $2q_{max}$ = 124.2°, 3454 independent intensities, 2850 observed (I > 1.00s (I)), T = 296K, R = 0.101, R_w = 0.142, GOF = 3.14, maximum residual electron density 0.39eÅ^{-3}. The X-ray data were collected on a Rigaku AFC7R four-circle diffractometer, using w/2q scan mode. All calculations were performed with the crystallographic software package teXsan (Molecular Structure Corporation, 1985, 1992). The structures were solved by direct methods[15] and subsequent Fourier recycling[16], and refined by full-matrix least-squares refinement against |F|, with all hydrogen atoms fixed at the calculated positions. A linear decay and empirical absorption corrections were applied[17].

4-3 Results and disccusion

Single-crystal-to-single-crystal enantioselective [2+2]photodimerization of coumarin 1a in

the 1:1 inclusion complex with (*R,R*)-(-)-3a

When a solution of a 1:1 mixture of **1a** and (-)-**3a** in AcOEt-hexane was kept at room temperature for 3 h, a 1:1 inclusion complex (**12**) was obtained as colorless needles.[4] Irradiation of **12** in the solid state with a 400 W high-pressure Hg lamp (Pyrex filter, room temperature, 4 h) gave a 2:1 complex (**13**) of (-)-**3a** with (-)-**6a**. After photoirradiation, the crystals were still clear and the reaction proceeded in a single-crystal-to-single-crystal manner throughout the reaction. The (–)-*anti*-head-to-head dimer (**6a**) was isolated by replacement of the guest (**6a**) with DMF. When the 2:1 complex (**13**) was recrystallized from DMF-H_2O (5:1), a 1:1 complex of (-)-**3a** with DMF was obtained as colorless needles in 99% yield. Concentration of the filtrate left the optically pure (–)-*anti*-head-to-head dimer (**6a**) which was isolated as colorless prisms in 89% yield. The optical purity of (-)-**6a** was determined by comparison of the $[a]_D$ value of enantiomerically pure **6a**.[12]

This result shows that two molecules of **1a** are arranged in charily related position, which gives the optically active *anti*-head-to-head dimer (**6a**) by [2+2] photodimerization. This chiral arrangement of the achiral molecule **1a** in the inclusion complex (**12**) can easily be detected by CD spectral measurement of its Nujol mull. The 1:1 complex of **1a** with (+)- and (-)-**3a** showed CD spectra with a mirror-imaged relation. (Fig. 1) After photoirradiation, the CD absorptions of **12** at 225, 275, 300 and 330 nm disappeared, and the new CD absorption due to **13** at 240 nm appeared. The photodimerization of **12** was also followed by measurement of IR spectra as Nujol mulls. Upon photoirradiation, the nCO absorption of **1a** in **12** at 1700 cm^{-1} decreased gradually and finally disappeared after 4 h, and new nCO absorption due to **6a** in **13** appeared at 1740 cm^{-1}.

The single-crystal-to-single-crystal nature and the steric course of the photodimerization of coumarin **1a** to (-)-anti-head-to-head dimer **3a** in the inclusion complex **12** were investigated by X-ray crystallographic analysis and X-ray powder diffraction spectroscopy. Crystal data are listed in Table 1. X-ray crystallographic analysis showed that two molecules of **1a** were arranged by forming a hydrogen bond between the C40=O6 of **1a** and the O4-H of **3a** in the direction which gave the *anti*-head-to-head dimer (**6a**) by photodimerization and the mo-

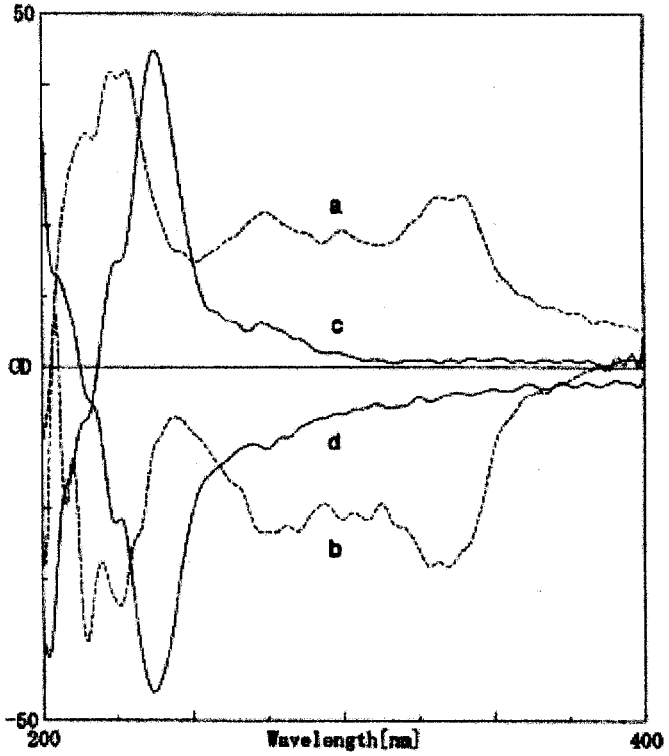

Fig. 1 CD spectra in Nujol mulls: (a) a 1:1 complex of **1a** with (+)-**3a**; (b) a 1:1 complex of **1a** with (-)-**3a**; (c) a 2:1 complex of (+)-**3a** with (+)-**6a**; (d) a 2:1 complex of (-)-**3a** with (-)-**6a**.

Table 1 Crystallographic Data for a 1:1 complex (**12**) of **1a** with (-)-**2a**, a 2:1 complex (**13**) of (-)-**2a** with (-)-**3a**, a 1:1 complex (**14** of **1b** with (-)-**2b**, a 2:1 complex (**15**) of (-)-**2b** with (+)-**3b**

compound	(12) monomer	(13) dimer	(14) monomer	(15) dimer
Formula	$C_{40}H_{36}O_6$	$C_{40}H_{36}O_6$	$C_{42}H_{38}O_5S_1$	$C_{42}H_{38}O_5S_1$
Crystal System	monoclinic	monoclinic	monoclinic	monoclinic
Space Group	*C2*	*C2*	$P2_1$	$P2_1$
a / Å	35.59((4)	32.80(3)	10.235(2)	10.371(3)
b / Å	9.489(4)	9.467(3)	35.78(1)	34.70(2)
c / Å	10.03(1)	10.360(4)	9.422(2)	9.414(3)
β /	102.70(4)	100.27(7)	91.00(2)	91.38(3)
V / Å^3	3305(4)	3164(2)	3449(1)	3387(2)
Z	4	4	4	4
*D*calc	1.23	1.29	1.26	1.28
No. of used refractions	1291	1962	4990	4178
R	0.101	0.114	0.065	0.078
temp. / °C	room	room	-50	-50

lecular aggregation with 3.59 and 3.42 Å were short enough contact ,which should react easily and topochemically.[8] After photoirradiation, the bond distances of the cyclobutane ring connecting C38-C38* and C39-C39* are 1.6 and 1.57 Å, respectively. (Fig. 2, 3)

The crystal-to-crystal nature of this reaction was also confirmed by X-ray powder diffraction spectroscopy. X-ray powder diffraction patterns has been recorded by a Rigaku X-ray diffractometer RINT 2000 with a divergence slit of 1 °, and an anti-scatter slit of 1 ° and a receiving slit of 0.15mm. A step scan with 2θ =3~30° and a 0.02° step size, Cu-*K*a radiation and a scan speed of 4°/min was used.

In the inclusion compounds **12** and **13**, the peaks at 2θ =8.90, 9.92 disappeared, and new peaks at 2θ =5.36, 8.46, 10.78 appeared during UV irradiation. After irradiation for 4 h, the original crystal structure was converted almost completely to the new structure. Remarkably, the peak of 2θ =9.92 (interplanar spacing of (400)) corresponding to 1/4 of the length of *a* axis

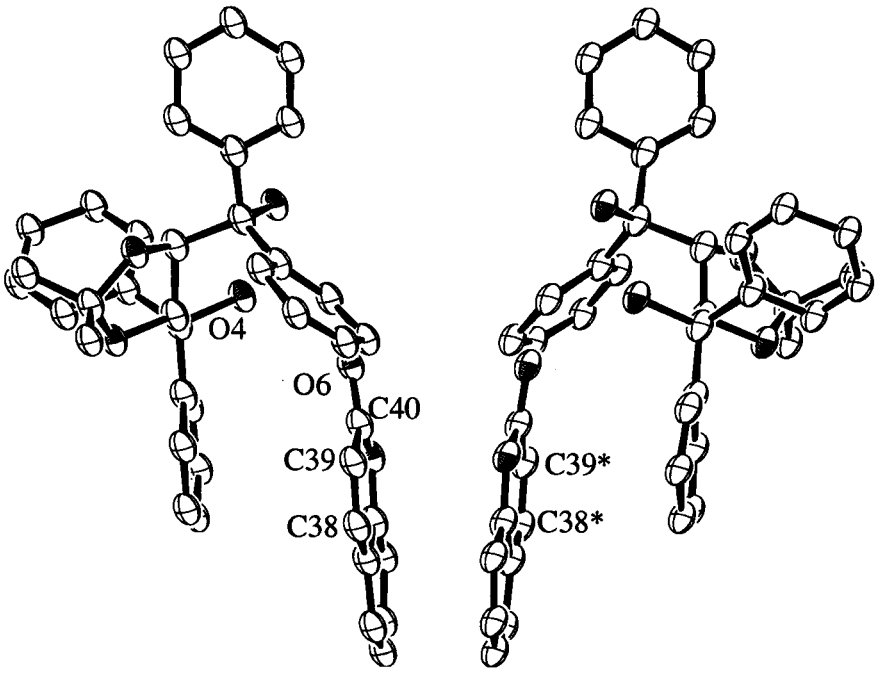

Fig. 2 ORTEP drawing of the molecular structure of a 1:1 complex (**12**) of **1a** with (-)-**2a** :viewed along the *a* axis. All hydrogen atoms are omitted for clarity. The hydrogen bonding are shown by dot lines.

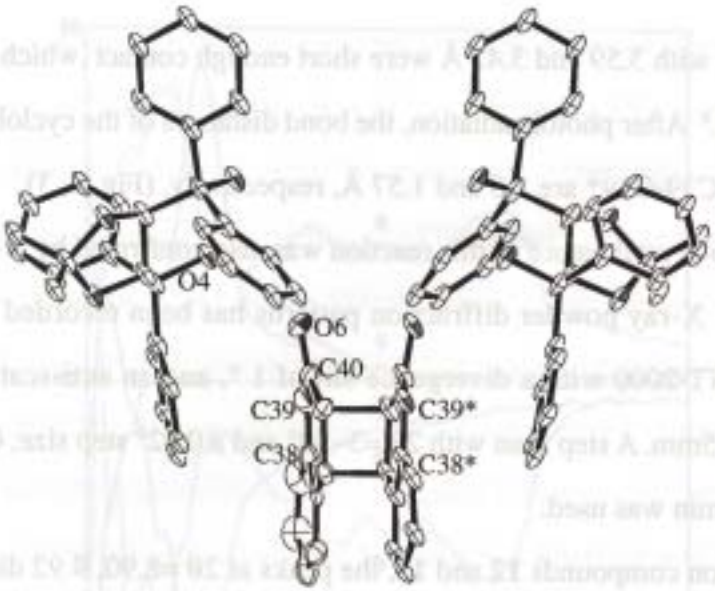

Fig. 3 ORTEP drawing of the molecular structure of a 2:1 complex (**13**) of (-)-**2a** with (-)-**3a** viewed along the *a* axis. All hydrogen atoms are omitted for clarity. The hydrogen bonding are shown by dot lines.

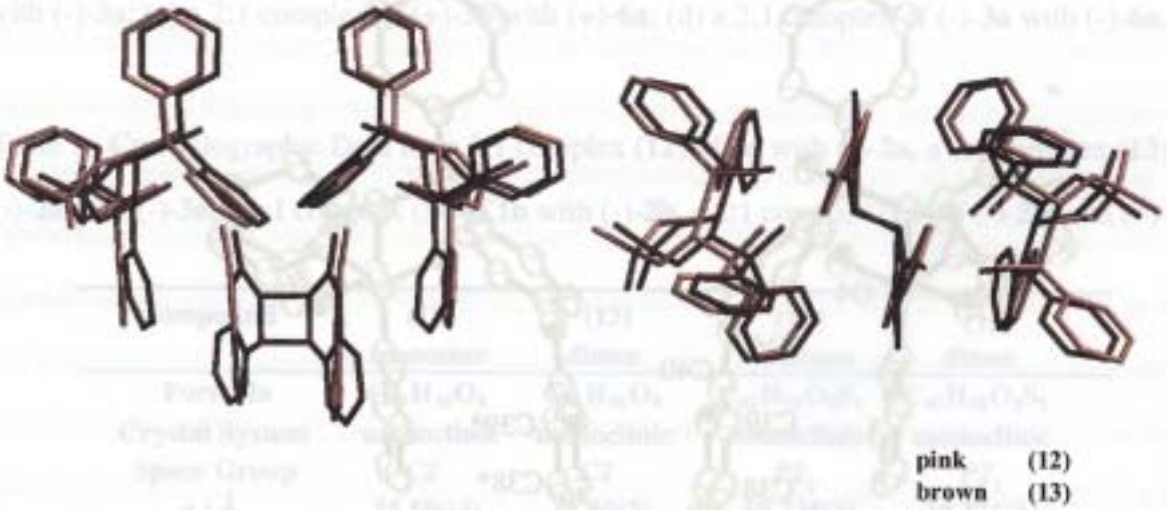

Fig. 4 Superposition of monomer and dimer conformation:
A 1:1 complex (**12**) of **1a** with (-)-**2a** (in pink) and a 2:1 complex (**13**) of (-)-**2a** with (-)-**3a** (in brown) , left is viewed along the *c* axis and right is viewed along the *b* axis. left is viewed along the *a* axis and right is viewed along the *c* axis. All hydrogen atoms The hydrogen bonding are shown by dot lines. This drawing was prepared by the program MIDASPLUS

shifted to 2q =10.78. The latter peak corresponds to the interplanar spacing of (400) for the 2:1 complex **13** (Fig. 5).

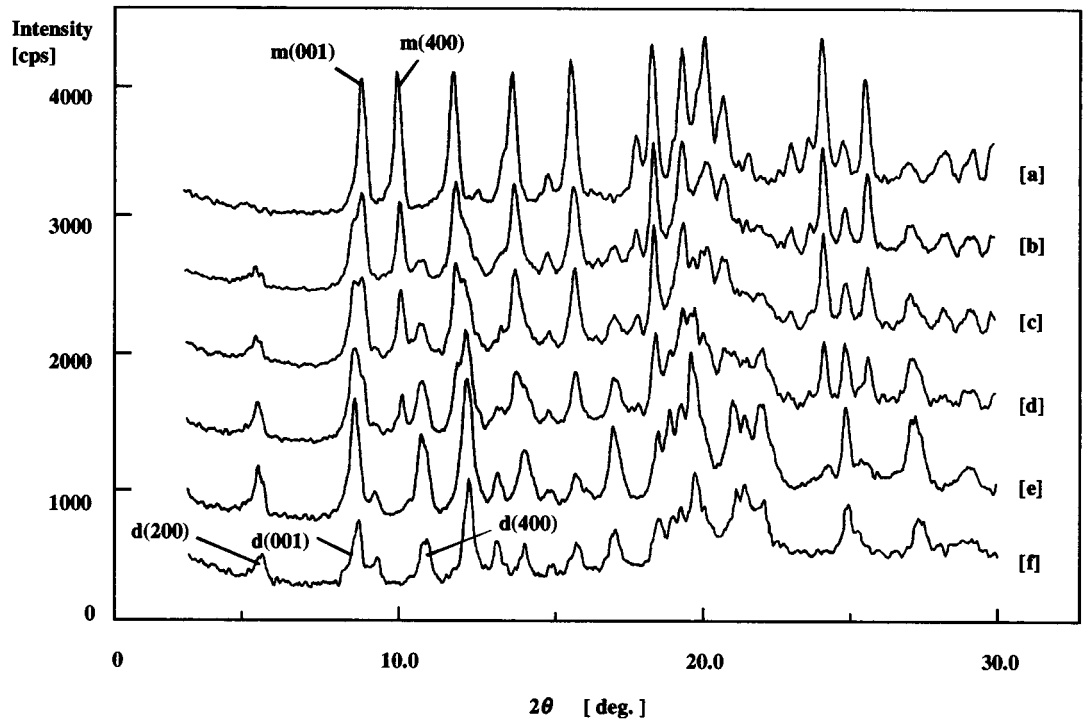

Fig. 5 X-ray powder diffraction patterns of (a) a 1:1 complex(**12**) of **1a** with (-)-**2a** (b) after UV irradiation for 10min (c) after UV irradiation for 30min (d) after UV irradiation for 90min (e) after UV irradiation for 4hr (f) a 2:1 complex(**13**) of (-)-**2a** with (-)-**3a** m(001) and m (400) in [a] are the mirror indices for complex(**12**). d(200) ,d (001) and d(400)in [f] are the mirror indices for complex(**13**).

The difference between molecular structures and crystal structures of **12** ~ **13** were shown in Fig. 4 and Fig. 6, respectively. As seen in Fig. 3, the cyclobutane ring forms approximately along the *a* axis. This corresponds well to the anisotropic changes in the lattice constants.

On the host molecule, it is revealed in Fig. 4 that there is not so much movement, though molecular structure of the cumarin moiety is changed largely with the formation of cyclobutane ring. The creation of C-C bond to cyclobutane effects a slight change in the cell dimensions, but

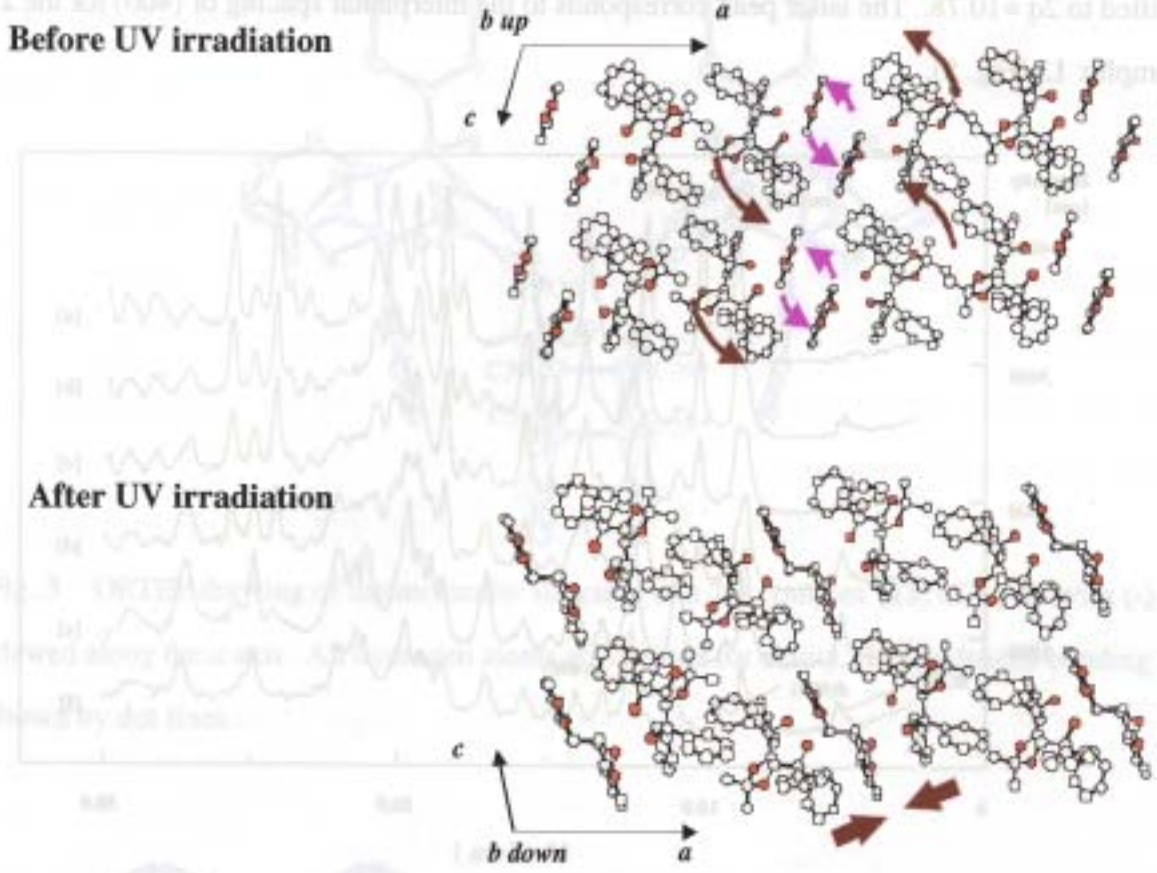

Fig. 6 Comparison of the crystal structures for complex(**4**) and (**5**): before and after UV irradiation. For clarity, hydrogen atoms are not shown .

leads to the reduction of the C-C distance (ca.1.9 Å) in **13** (1.6 and 1.57 Å) as compared to that of the starting **12**.

It is revealed that the one of phenyl groups of host molecule of **12** and **13** have a contact to coumarin ring through π–π interactions. The coumarin ring moves toward in direction from *ac* axis to *a* axis vertically with the formation of cyclobutane after photoirradiation. (pink (**12**) and brown (**13**) in Fig. 4 right)

In the crystal structure of **12** and **13**, these molecular arrangement greatly changes, and the whole transfer is occurred along the *ac* axis, and the lattice constant is not almost different from -0.02 Å in *b* axis through the reaction, and the change of lattice constant is 2.45 Å and +0.35 Å in *a* and *c* axis, respectively. Through the reaction, the change of the *ac* axis is related

to the value of *b* in the crystal structure. The description of causing large change of *b*, that is -2.43°, is explicable, in the reaction. (Fig. 6).

Single-crystal-to-single-crystal enantioselective [2+2]photodimerization of thiocoumarin 1b in the 1:1 inclusion complex with (*R,R*)-(-)-3b

The enantioselective photodimerization of thiocoumarin (**1b**) to optically pure (+)-*anti*-head-to-head dimer (**6b**) in the 1:1 inclusion complex (**14**) of **1b** with (-)-**3b** was also found to proceed in a single-crystal-to-single-crystal manner. For example, when a mixture of thiocoumarin **1b** and optically active host compound (*R,R*)-(-)-**3b** in butyl ether was kept at room temperature for 12 h, a 1:1 inclusion complex **14** of **1b** with (-)-**3b** was obtained as colorless needles.[5] Photoirradiation of **14** in the solid state (400 W high-pressure Hg lamp, Pyrex filter, room temperature, 2 h) gave a 2:1 complex (**15**) of (-)-**3b** with (+)-**6b**, quantitatively. (+)-**6b** of 100% ee was isolated in 73% yield by column chromatographic separation. The crystal-to-crystal nature of this reaction was also confirmed by X-ray powder diffraction spectroscopy.

Chiral transformation of the achiral molecule **1b** in the inclusion complex (**14**) can easily be detected by CD spectral measurement of its Nujol mull. The 1:1 complex of **1a** with (+)- and (-)-**3b** showed CD spectra with a mirror-imaged relation. (Fig. 7) After photoirradiation, the CD absorptions of **14** at 260 and 320 nm disappeared, and the new CD absorption due to **15** at 270 and 330 nm appeared.

The single-crystal-to-single-crystal nature and the steric course of the photodimerization of thiocoumarin **1b** to (+)-anti-head-to-head dimer **6a** in the inclusion complex **14** were investigated by X-ray crystallographic analysis and X-ray powder diffraction spectroscopy. Two molecules of **1b** in a 1:1 inclusion complex **14** of **1b** with (-)-**3b** are related to a pseudo two-fold axis along *c* axis. (Fig. 8) C75=O9, C84=O10 of **1b** and the O4-H, O7-H of **3b** form a hydrogen bond in the direction which gives the *anti*-head-to-head dimer (**6b**). (Fig. 9) The distance between the two ethylenic double bonds is enough short (3.73 and 3.41 Å) to react easily and topochemically.[8] After photoirradiation, the bond distances of the cyclobutane ring connecting C74-C83 and C73-C82 are 1.60 and 1.60 Å, respectively. The distance of atoms formed hydro-

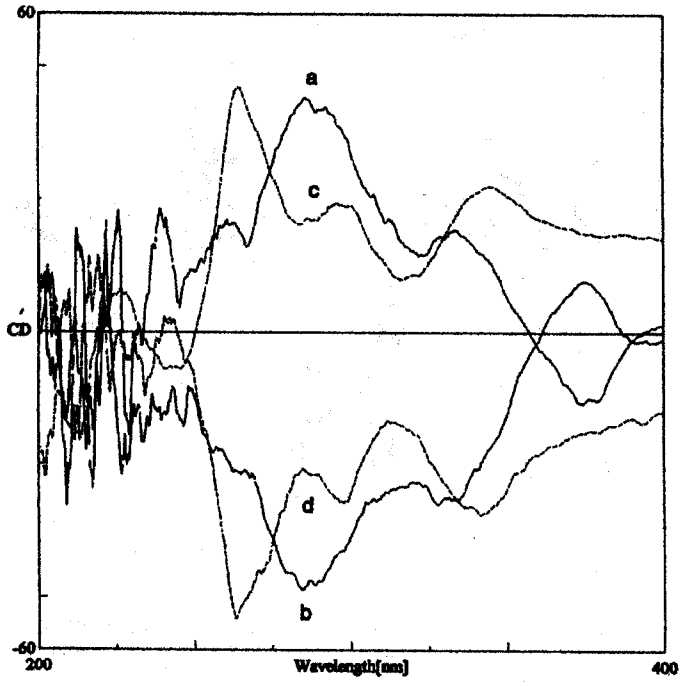

Fig. 7 CD spectra in Nujol mulls: (a) a 1:1 complex of **1b** with (+)-**3a**; (b) a 1:1 complex of **1b** with (-)-**3a**; (c) a 2:1 complex of (+)-**3a** with (-)-**6b**; (d) a 2:1 complex of (-)-**3a** with (+)-**6b**.

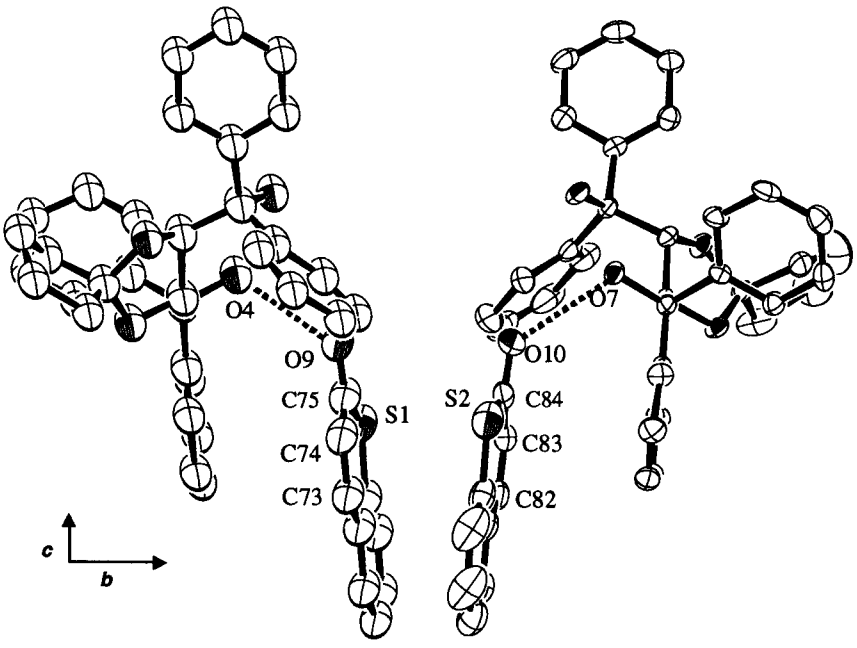

Fig. 8 ORTEP drawing of the molecular structure of a 1:1 complex (**14**) of **1b** with (+)-**2b** viewed along the *a* axis. All hydrogen atoms are omitted for clarity. The hydrogen bonding are shown by dot lines.

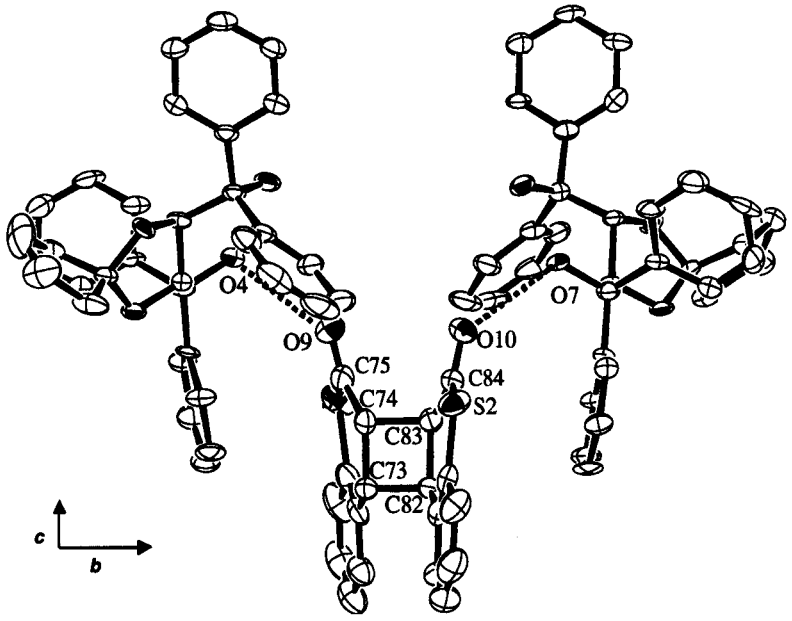

Fig. 9 ORTEP drawing of the molecular structure of a 2:1 complex (**15**) of (-)-**2b** with (+)-**3b** viewed along the *a* axis. All hydrogen atoms are omitted for clarity. The hydrogen bonding are shown by dot lines.

gen bond are (O4-H.... O9= C75 , O7-H...O10 = C84) are 2.81 and 2.77 Å in a 1:1 inclusion complex **14** of **1b** with (-)-**2b** , respectively. In a 2:1 complex **15** of (-)-**2b** with (+)-**3b** , these corresponding distances are 2.92 and 2.85 Å. These distances can cause hydrogen bonding, while the distances after photoirradiation are rather longer than thoses before irradiation.

In the inclusion compounds **14**, **15**, the peaks at 2θ =8.64, 9.42 disappeared, and new peaks at 2θ =5.20, 8.76, 10.32 appeared during UV irradiation. After irradiation for 4 h, the original crystal structure had been transformed almost completely to the new structure. The peak corresponding to 1/4 length of *b* axis (interplanar spacing of (040)) had shifted from 2θ =9.42 to 2θ =10.32. The latter peak is equal to the interplanar spacing of (040) for the 2:1 complex **15**. (Fig. 10) From these data, we conclude that the photodimerization of the 1:1 complex **14** proceeded in a single-crystal-to-single-crystal manner.

During the conversion of **14** to **15**, a similar conformational change were observed in a single crystal. From the superposition of molecular structure, thiocoumarin ring and phenyl group are stacked to synchronous transform in the case of **12** to **13**, and little rotation occur in crystal

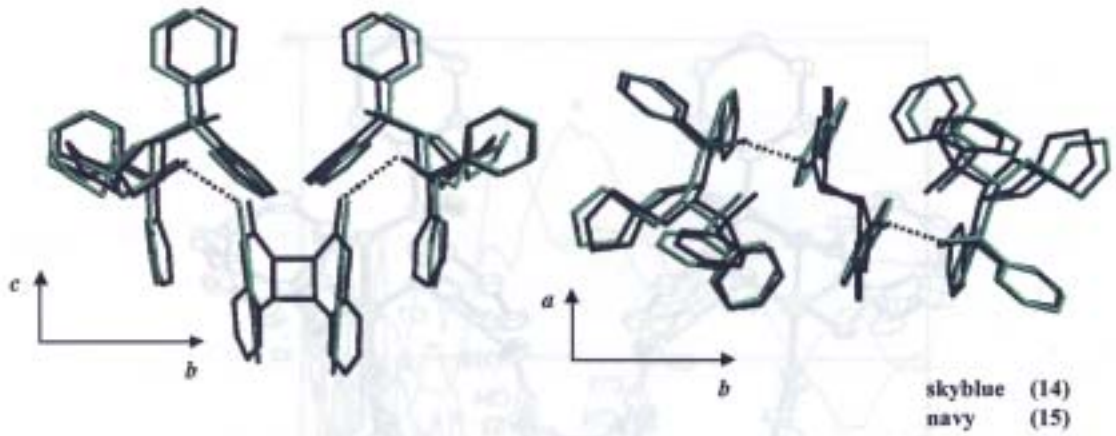

Fig. 10 Superposition of monomer and dimer conformation:

A 1:1 complex (**14**) of **1b** with (-)-**2b** (in skyblue), a 2:1 complex (**15**) of (-)-**2b** with (+)-**3b** (in navy), left is viewed along the *a* axis and right is viewed along the *c* axis. All hydrogen atoms are omitted for clarity. The hydrogen bonding are shown by dot lines. This drawing was prepared by the program MIDASPLUS

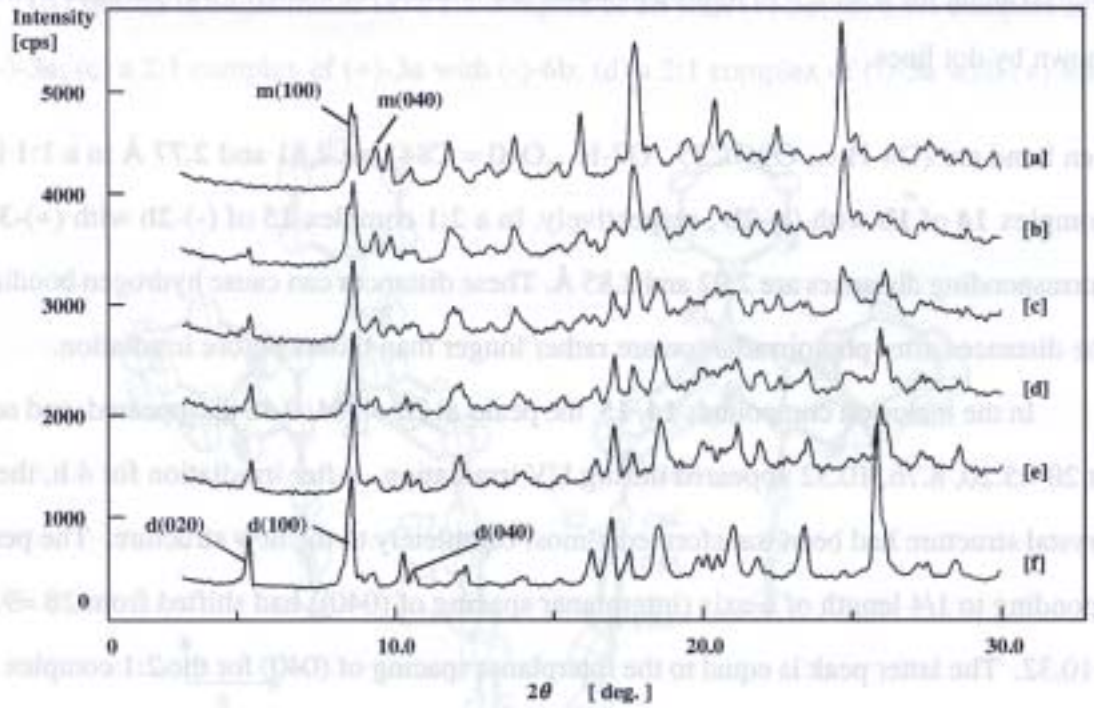

Fig. 11 X-ray powder diffraction patterns of (a) a 1:1 complex (**14**) of (-)-**1b** with (+)-**3b** (b) after UV irradiation for 20min (c) after UV irradiation for 20min (d) after UV irradiation for 20min(e) a 2:1 complex (**15**) of (-)-**2b** with (+)-**3b**

m(100) and m (040) in [a] are the mirror indices for complex(**14**).

d(020) ,d (100) and d(040)in [f] are the mirror indices for complex(**15**).

state.

In the crystal structure , the changes in lattice constants from **14** to **15** were -0.136 Å and -0.008 Å for *a* and *c*, respectively, they were almost equal after the photoirradiaton. The length of b axis , however, decreased 1.08 Å with creation of cyclobutane. The molecular arrangement from **14** to **15** changed less than from **12** to **13**. The direction of their rotation is almost parallelly in *b* axis, and the change of angle is also small with +0.38 ° (Fig. 11)

This situation corresponds well to the anisotropic alteration in tne lattice constant. The degree of change in the crystal structure also influences photodimerization reaction rate in the solid state. Their molecular rearrangement corresponds to their photoreaction rate.

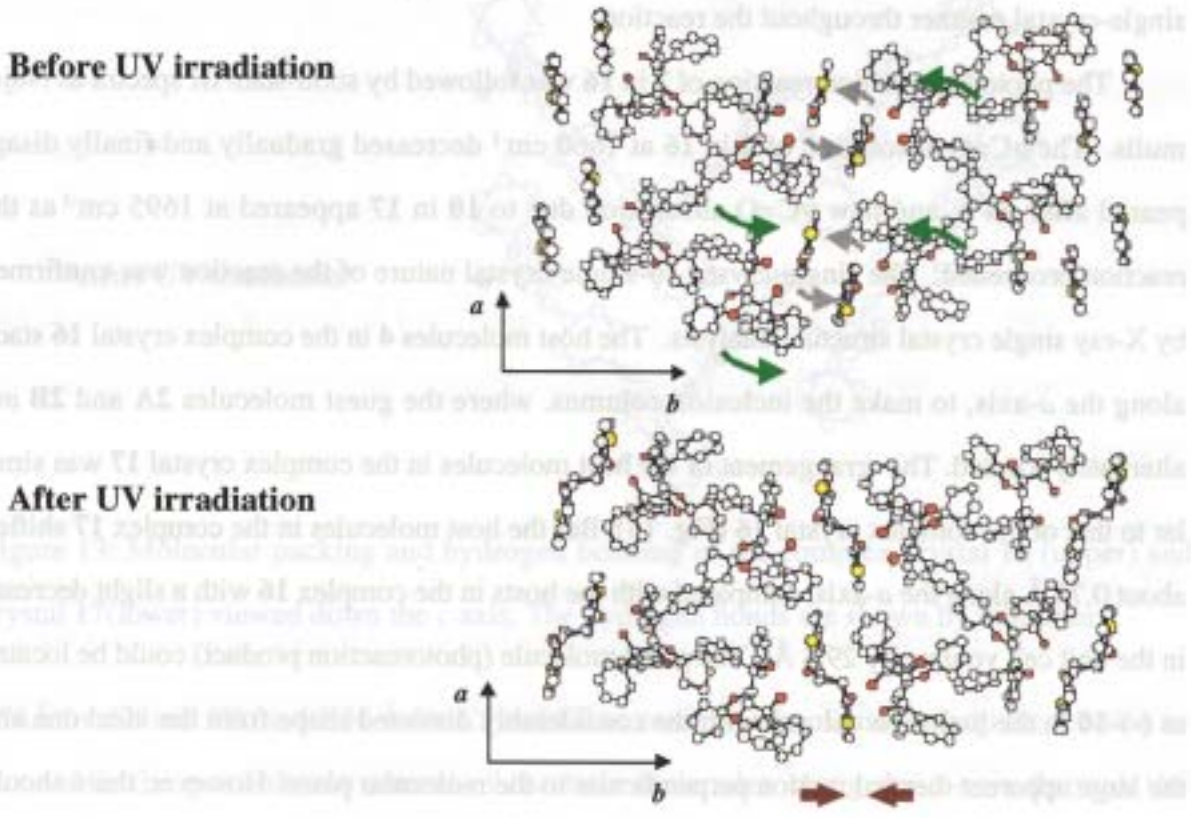

Fig. 12 Comparison of the crystal structures for complex(**14**) and (**15**): before and after UV irradiation. For clarity, hydrogen atoms are not shown.

Single-crystal-to-single-crystal enantioselective [2+2]photodimerization of cyclohex-2-enone in the inclusion crystals with (-)-1,4-bis[3-(o-chlorophenyl)-3-hydroxy-3-phenylprop-1-ynyl]benzene

A solution of (-)-**4** and **2** in ether-hexane (1:1) was kept at room temperature for 6 h to give a 1:2 complex (**16**) of (-)-**4** and **2** as colorless prisms in 91% yield.[6] Photoirradiation of single-crystals of **16** (mp 90-95 °C) with 400 W high-pressure Hg-lamp through Pyrex filter for 24 h gave single-crystals of a 2:1 complex **17** (mp 79-84 °C) of **4** with (-)-**10**, which upon distillation in vacuo to give (-)-**10** of 46% ee in 75% yield.[6] When the reaction was carried out at –78 °C in the solid state for 30 h, (-)-**10** of 58% ee was obtained in 55% yield. After photoirradiation, the crystal was still clear and the reaction proceeded in a single-crystal-to-single-crystal manner throughout the reaction.

The photodimerization reaction of **2** in **16** was followed by solid-state IR spectra as Nujol mulls. The nC=O absorption of **2** in **16** at 1660 cm^{-1} decreased gradually and finally disappeared after 24 h, and new νC=O absorption due to **10** in **17** appeared at 1695 cm^{-1} as the reaction proceeded. The single-crystal-to-single-crystal nature of the reaction was confirmed by X-ray single crystal structure analysis. The host molecules **4** in the complex crystal **16** stack along the *a*-axis, to make the inclusion columns, where the guest molecules **2A** and **2B** are alternately located. The arrangement of the host molecules in the complex crystal **17** was similar to that of the complex crystal **16** (Fig. 13). But the host molecules in the complex **17** shifted about 0.73 Å along the *a*-axis, compared with the hosts in the complex **16** with a slight decrease in the unit cell volume by 29.4 $Å^3$. The guest molecule (photoreaction product) could be located as (-)-**10** in the inclusion column with the considerably distorted shape from the ideal one and the large apparent thermal motion perpendicular to the molecular plane. However, there should be (+)-**2** as a minor product in the complex crystal **17**, since the reaction product consists of (-)-**2** and (+)-**2** in about 3:1 ratio.

Fig. 14 shows the arrangement of the guests (**2A**, **2B** and **2B***) and the host in the complex **16**. The C4-C5 bond in **2A** makes a short contact with the C7-C8 in **2B** (C4—C8 =3.99, C5—C7 = 4.16 Å) giving the reaction product of (-)-**2**. The distances between the π orbital lobe apexes are

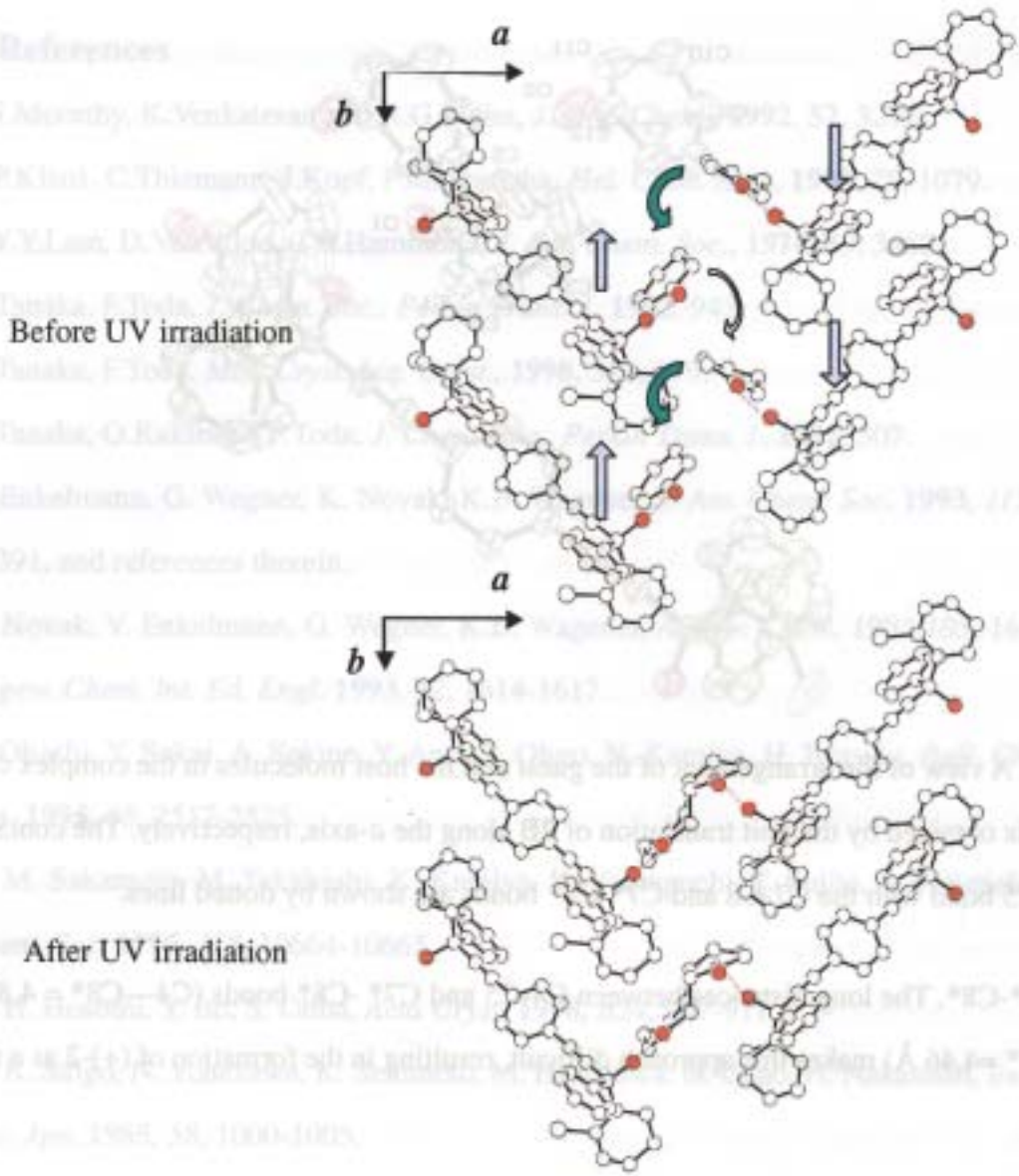

Figure 13: Molecular packing and hydrogen bonding of the complex crystal **16** (upper) and crystal **17**(lower) viewed down the *c* axis. The hydrogen bonds are shown by thin lines.

1.76Å for C4 and C8, and 1.56 Å for C5 and C7 atoms.[14] Another factor to help the reaction to proceed is the possible movement of the host molecules along the *a*-axis through the photodimerization reaction. The comparison of the crystal structure of **16** with that of **17** shows that hosts **4A** and **4B** can move parallel to the *a*-axis, but in the reverse direction, giving the close approach (about 1.4 Å) of **2A** and **2B**, which are hydrogen bonded to **4A** and **4B**, respectively. The mirror image ((+)-**2**) of the major product will be given if the molecule **2A** rotates toward **2B*** along the axis joining C3 and C6 atoms, and C4-C5 bond of **2A** approaches to react

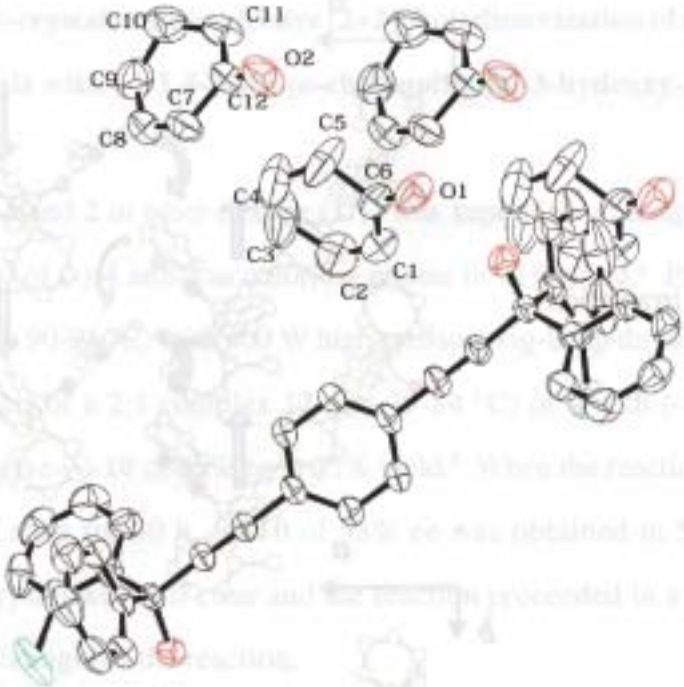

Fig. 14 A view of the arrangement of the guest and the host molecules in the complex crystal **16**. **2B*** is obtained by the unit translation of **2B** along the *a*-axis, respectively. The contacts of the C4-C5 bond with the C7-C8 and C7*-C8* bonds are shown by dotted lines.

with C7*-C8*. The long distances between C4-C5 and C7* -C8* bonds (C4—C8* = 4.82 and C5—C7* =4.46 Å) makes this approach difficult, resulting in the formation of (+)-**2** as a minor product.

4-4 Conckusion

Single-crystal-to-single-crystal enantioselective [2+2] photodimerization reactions of coumarin (**1a**), thiocoumarin (**1b**) and cyclohex-2-enone (**2**) were found to proceed efficiently in inclusion complexes with (*R,R*)-(-)-*trans*-bis(hydroxydiphenylmethyl)-2,2-dimethyl-1,3-dioxacyclopentane (**3a**), (*R,R*)-(-)-*trans*-2,3-bis(hydroxydiphenylmethyl)-1,4-dioxaspiro[4.4]nonane (**3b**), and (-)-1,4-bis[3-(o-chlorophenyl)-3-hydroxy-3-phenylprop-1-ynyl]benzene (**4**), respectively. Through these reactions, (-)-anti-head-to-head dimer **6a**, (+)-anti-head-to-head dimer **6b** and (-)-syn-trans dimer **10** were obtained in 100, 100 and 48% ee, respectively.

4-5 References

1. J.N.Moorthy, K.Venkatesan and R.G.Weiss, *J. Org. Chem.*, **1992**, 57, 3292.
2. C.P.Klaus, C.Thiemann, J.Kopf, P.Margaretha, *Hel. Chim. Acta*, **1995**, 78, 1079.
3. E.Y.Y.Lam, D.Valentine, G.S.Hammond, *J. Am. Chem. Soc.*, **1976**, 89, 3482.
4. K.Tanaka, F.Toda, *J. Chem. Soc., Perkin Trans. 1*, **1992**, 943.
5. K.Tanaka, F.Toda, *Mol. Cryst. Liq. Cryst.*, **1998**, 313, 179.
6. K.Tanaka, O.Kakinoki, F.Toda, *J. Chem. Soc., Perkin Trans. 1*, **1992**, 307.
7. V. Enkelmann, G. Wegner, K. Novak, K.B. Wagener, *J. Am. Chem. Soc.* **1993**, *115*, 10390-10391, and references therein.
8. K. Novak, V. Enkelmann, G. Wegner, K.B. Wagener, *Angew. Chem.* **1993**,*105*, 1678-1680; *Angew. Chem. Int. Ed. Engl.* **1993**, *32*, 1614-1617.
9. Y. Ohashi, Y. Sakai, A. Sekine, Y. Arai, Y. Ohgo, N. Kamiya, H. Iwasaki, *Bull. Chem. Soc. Jpn.* **1995**, *68*, 2517-2525.
10. M. Sakamoto, M. Takahashi, K. Kamiya, K. Yamaguchi, T. Fujita, S. Watanabe, *J. Am. Chem. Soc.* **1996**, *118*, 10664-10665.
11. H. Hosomi, Y. Ito, S. Ohba, *Acta Cryst.* **1998**, *B54*, 907-911.
12. K. Saigo, N. Yonezawa, K. Sekimoto, M. Hasegawa, K. Ueno, H. Nakanishi, *Bull. Chem. Soc. Jpn.* **1985**, *58*, 1000-1005.
13. K. Tanaka, F. Toda, *Mol. Cryst. Liq. Cryst.* **1998**, *313*, 179-184; C. P. Klaus, C. Thiemann, J. Kopf, P. Margaretha, *Helv. Chim. Acta.* **1995**, *78*, 1079-1082; J. Kopf, H. Maelger, C. Thiemann, P. Margaretha, *Acta Cryst.* **1994**, *C50*, 1922-1924.
14. S.K. Kearsley, In Organic Solid State Chemistry, (ed. G.RÅDDesiraju), Elsevier. Amsterdam, pp69, 1987.
15. G.M. Sheldrick, Crystallographic Computing 3 (ed. G.M. Sheldrick; C. Kruger; R. Goddard) Oxford University Press, **1985**, 175-189.
16. P.T. Beurskens, G. Admiraal, G. Beurskens, W.P. Bosman, R. de Gelder, R. Israel, J.M.M. Smits, The DIRDIF-94 program system, Technical Report of the Crystallography Laboratory, **1994**, University of Nijmegen, The Netherlands.
17. A.C.Y. North, D.C. Philips, F.S. Mathews, Acta Crystallographica, 1968, **A24**, 351.

Conclusion

This thesis deals with the studies of the relationship between structure, reactivity and mechanism in the crystal phase reaction.

In Chapter 1, the author showed crystal structures and the solid-state polymerization of 1,4-bis(5-hydroxypenta-1,3-diynyl)benzene (1), 1,2-bis(5-hydroxypenta-1,3-diynyl)benzene (2) and 1-(5-hydroxypenta-1,3-diynyl)-4-ethynylbenzene (3) . The crystal structure of 1 depends on recrystallization solvents. The crystals obtained from acetone-benzene mixtures polymerize when irradiated with γ-rays or heated. The colourless crystals become black and insoluble in common organic solvents. Only one of the butadiynyl groups participates in the radiation-induced polymerization, whereas the both, in the thermal polymerization. Polymerization does not occur for the crystals obtained from pure acetone. The polymerization reactivities were correlated to the crystal structures. Polymerizable crystals were not obtained from 2. The arrangement of the butadiynyl groups in the crystals of 2 is unfavorable for the polymerization. The crystals of 3, obtained from hexane-acetone mixtures, polymerize upon γ-irradiation but not upon heating. In the radiation-induced polymerization of 3, the propagation by the ethynyl and butadiynyl groups is considered to proceed independently along the different crystal axes. The ethynyl group is more reactive than the butadiynyl group because of the shorter intermolecular carbon-carbon distance responsible for the polymerization. The difference in reactivity toward heating between 1 and 3 may also be attributed to the intermolecular carbon-carbon distances of the butadiynyl groups.

In Chapter 2, the author revealed the crystal structures by X-ray crystal analysis that single crystals of 1-alkylthymine (carbon numbers of the alkyl chain were 8, 11, 12, 13, 14, and 16) were obtained from *N, N*-dimethylformamide (DMF) solution as plates. The terminal methyl group of the alkyl chain was found to approach to the double bond of the thymine base in the crystal. The thymine bases in these crystals did not give the photodimer by UV irradiation, while the crystals obtained from ethyl acetate and acetonitrile gave the photodimer as reported previously. The terminal methyl group of the alkyl chain was concluded to inhibit the rotation of

the thymine bases in crystal, which made the crystal from DMF inactive for the photodimerization.

In Chapter 3, the author clarified the crystal structure and photodimerization of 1-alkylthymine in single crystals. Length of alkyl chains in 1-alkylthymine affected on crystal structure and photodimerization in single crystal. 1-Alkylthymine gave two types of crystals, **Type 1** and **Type 2** depending on length of alkyl chains and solvent used. This paper deals with **Type 1** crystal, where thymine bases form plates by hydrogen bonding. UV irradiation at 280 nm on **Type 1** crystals of 1-alkylthymine gave cyclobutane type photodimers. Crystals of 1-pentylthymine (**C 5**), 1-nonylthymine (**C 9**), and 1-decylthymine (**C 10**) gave *a trans-syn* photodimer, but 1-octylthymine (**C 8**) crystal gave a *trans-anti* photodimer. Alkyl chains played an important role in forming different isomers of photodimers.

In Chapter 4, the author revealed that single-crystal-to-single-crystal enantioselective [2+2] photodimerization reactions of coumarin (**1a**), thiocoumarin (**1b**) and cyclohex-2-enone (**2**) proceed efficiently in inclusion complexes with (*R,R*)-(-)-*trans*-bis(hydroxydiphenylmethyl)-2,2-dimethyl-1,3-dioxacyclopentane (**3a**), (*R,R*)-(-)-*trans*-2,3-bis(hydroxydiphenylmethyl)-1,4-dioxaspiro[4.4]nonane (**3b**), and (-)-1,4-bis[3-(o-chlorophenyl)-3-hydroxy-3-phenylprop-1-ynyl]benzene (**4**), respectively. Through these reactions, (-)-anti-head-to-head dimer **6a**, (+)-anti-head-to-head dimer **6b** and (-)-syn-trans dimer **10** were obtained in 100, 100 and 48% ee, respectively. The single-crystal-to-single-crystal nature and the steric course of the photodimerization of coumarin **1a** to (-)-anti-head-to-head dimer **3a** in the inclusion complex **12** were investigated by X-ray crystallographic analysis and X-ray powder diffraction spectroscopy. The author revealed that the one of phenyl groups of host molecule of **12** and **13** have a contact to coumarin ring through π–π interactions. The coumarin ring moves toward in direction from *ac* axis to *a* axis vertically with the formation of cyclobutane after photoirradiation.

List of Publications

1) Single-crystal-to-single-crystal enantioselective photodimerization of coumarin and thiocoumarin in inclusion crystals with chiral host compounds
K. Tanaka, F. Toda, E. Mochizuki, N. Yasui, Y. Kai, I. Miyahara, and K. Hirotsu,
Angew. Chem. Int. Ed., **38**, 3523-3525 (1999).

2) Intramolecular photodimerization of bisthymine compounds
Y. Inaki, E. Mochizuki, H. Donoue, M. Miyata, N. Yasui, and Y. Kai,
J. Photopolym. Sci. Technol., **12**, 725-734 (1999).

3) Crystal structures and solid-state reactivities of 1,4- and 1,2-bis (5-hydroxypenta-1,3-diynyl)benzenes and 1-(5-hydroxypenta-1,3-diynyl)-4-ethynylbenzene
E. Mochizuki, Y. Shibamoto, K. Yano, N. Kanehisa, Y. Kai, S. Tagawa, and Y. Yamamoto,
J. Chem. Soc., Perkin Trans. 2, 155-159 (2000).

4) Structures and photodimerizations of 1-alkylthymine crystals obtained from *N, N*-dimethylformamide
E. Mochizuki, N. Yasui, Y. Kai, Y. Inaki, N. Tohnai, and M. Miyata,
Bull. Chem. Soc. Jpn., **73**, 1035-1041 (2000).

5) Reversible photodimerization of ester derivatives of thymine having long alkyl chain in solid film
E. Mochizuki, N. Yasui, Y. Kai, Y. Inaki, W. Yuhua, T. Saito, N. Tohnai, and M. Miyata,
Polym. J., **32**, 492-500 (2000).

6) Single-crystal-to-single-crystal enantioselective [2+2] photodimerization of coumarin, thiocoumarin and cyclohex-2-enone in the inclusion complexes with chiral host compounds
K. Tanaka, E. Mochizuki, N. Yasui, Y. Kai, I. Miyahara, K. Hirotsu, and F. Toda,
Tetrahedron, **56**, 6853-6865 (2000).

7) Crystal structure and photodimerization of 1-alkylthymine: Effect of long alkyl chain on isomer ratio of photodimer
Y. Inaki, E. Mochizuki, N. Yasui, M. Miyata, and Y. Kai,
J. Photopolym. Sci. Technol., **13**, 177-182 (2000).

8) Crystal structure of long alkyl 2-(thymin-1-yl)propionates: Style of hydrogen bonding and dependence on the alkyl chain length
E. Mochizuki, N. Yasui, Y. Kai, Y. Inaki, W. Yuhua, T. Saito, N. Tohnai, and M. Miyata,

List of Supplementary Publications

1) Synthesis of poly-L-glutamates containing 5-substituted uracil moieties
E. Mochizuki, Y. Inaki, and K. Takemoto,
Nucleic Acids Res., Sym. Ser., **16**, 121-124 (1985).

2) Effect of metal ions on the interaction of synthetic nucleic acid analogs
E. Mochizuki, Y. Inaki, and K. Takemoto,
J. Macromol. Sci., -Chem., **A24**, 353-356 (1987).

3) Synthesis and properties of polyamino acid derivatives containing nucleic acid bases and nucleosides
T. Wada, E. Mochizuki, Y. Inaki, and K. Takemoto,
Peptide Chem., **1987**, 41-44 (1987).

4) Nucleic acid analogs: Their specific interaction and applicability
K. Takemoto, E. Mochizuki, T. Wada, and Y. Inaki,
Biomimetic Polymers, 253-267 (1990).

5) Watersoluble synthetic nucleic acid analogs-polyethyleneimine derivatives containing nucleic acid bases-conformation and interaction with nucleic acids
T. Wada, E. Mochizuki, Y. Inaki, and K. Takemoto,
Nucleic Acids Res., Symp. Ser., **22**, 113-114 (1990).

6) Synthesis and interactioon of water soluble nucleic acid analogs
K. Takemoto, T. Wada, E. Mochizuki, and Y. Inaki,
Polym. Mater. Sci. Eng., **62**, 558-62 (1990).

7) Synthesis and interaction studies of oligo and polyamino acids derivatives containing nucleosides
T. Wada, E. Mochizuki, Y. Inaki, and K. Takemoto,
Nucleic Acids Res., Symp. Ser., **25**, 19-20 (1991).

8) Synthesis and interaction of water soluble nucleic acid analogs
K. Takemoto, T. Wada, E. Mochizuki and Y. Inaki,
Biotechnology and Polymers, **1991**, 31-45 (1991).

9) Synthesis and interaction studies of water soluble nucleic acid analogs containing serine as a spacer
T. Wada, N. Masumi, E. Mochizuki, Y. Inaki, and K. Takemoto,
Nucleic Acids Res., Symp. Ser., **27**, 115-116 (1992).

10) Immobilization of nucleoside on silica gel and specific separation of oligonucleotides
Y. Inaki, K. Matsukawa, H. Kawano, W. Hong, T. Wada, E. Mochizuki, and K. Takemoto,
Nucleic Acids Res., Symp. Ser., **27**, 29-30 (1992).

11) Photodimerization of thymine derivatives in ionomer matrixes
E. Mochizuki, K. Masuda, T. Wada, and Y. Inaki,
J. Photopolym. Sci. Technol., **6**, 131-132 (1993).

12) High performance liquid chromatographic separation of oligonucleotides using deoxyadenosine immobilized silica gel for stationary phase
Y. Inaki, K. Matsukawa, H. Wang, E. Mochizuki, T. Wada, and K. Takemoto,
Bunseki Kagaku, **42**, 99-105 (1993).

13) Synthesis and properties of oligolysine and oligoglutamic acid derivatives containing nucleosides and polyamino acids derivatives containing nucleosides
T. Wada, K. Okada, M. Nakamori, E. Mochizuki, and Y. Inaki,
Nucleic Acids Res., Symp. Ser., **29**, 79-80 (1993).

14) High performance liquid chromatographic separation of oligonucleotides using deoxyadenosine immobilized silica gel for stationary phase. Effect of the deoxyadenosine ligand concentration
Y. Inaki, Y. Ohsaki, H. Wang, K. Matsukawa, E. Mochizuki, and T. Wada,
Bunseki Kagaku, **42**, 825-30 (1993).

15) Synthesis and properties of water soluble poly-L- and -D-lysine derivatives containing nucleic acid bases
T. Wada, M. Nakamori, E. Mochizuki, and Y. Inaki,
Nucleic Acids Res., Symp. Ser., **31**, 135-136 (1994).

16) Photopolymerization and crystal structure of long alkyl thymine derivatives
N. Tohnai, T. Sugiki, E. Mochizuki, T. Wada, and Y. Inaki,
J. Photopolym. Sci. Technol., **7**, 91-92 (1994).

17) Remarkably wide range of bond distance adjustment of d9-d9 Pd-Pd interactions to change in coordination environment
T. Murahashi, T. Otani, E. Mochizuki, Y. Kai, and H. Kurosawa,
J. Am. Chem. Soc., **120**, 4536-4537 (1998).

18) Photodimerization of thymine derivatives in single crystal
N. Tohnai, Y. Inaki, M. Miyata, N. Yasui, E. Mochizuki, and Y. Kai,
J. Photopolym. Sci. Technol., **11**, 59-64 (1998).

19) Photodimerization of 1-alkylthymines crystallized from acetonitrile solution
N. Tohnai, Y. Inaki, M. Miyata, N. Yasui, E. Mochizuki, and Y. Kai,
Bull. Chem. Soc. Jpn., **72**, 1143-1151 (1999).

20) Photoreactive and inactive crystals of 1-alkylthymine derivatives
N. Tohnai, Y. Inaki, M. Miyata, N. Yasui, E. Mochizuki, and Y. Kai,
Bull. Chem. Soc. Jpn., **72**, 851-858 (1999).

21) Organometallic sandwich chains made of conjugated polyenes and metal-metal chains
T. Murahashi, E. Mochizuki, Y. Kai, and H. Kurosawa,
J. Am. Chem. Soc., **121**, 10660-10661 (1999).

22) Reversible interconversion between dinuclear sandwich and half-sandwich complexes: Unique dynamic behavior of a Pd-Pd moiety surrounded by an sp(2)-carbon framework
T. Murahashi, T. Nagai , Y. Mino , E. Mochizuki, Y. Kai, and H. Kurosawa,
J. Am. Chem. Soc., **123**, 6927-6928 (2001).

23) Synthesis and nonlinear properties of poly[1,4-bis(4-methylpyridinium)butadiyne triflate)]
K. Shiga, T. Inoguchi, K. Mori, K. Kondo, K. Kamada, K. Tawa, K. Ohta, T. Maruo, E. Mochizuki, and Y. Kai,
Macromol. Chem. Phy., **202**, 257-262 (2001).

Acknowledgements

The author is particularly grateful to express her sincere gratitude to Professor Yasushi Kai for his giving the author a chance to study on this field, helpful suggestion throughout this work. The author acknowledges the continuing encouragement of Professor Mikiji Miyata.

The authour also deeply grateful to Dr. Yoshiaki Inaki for their useful advice and continuous encouragement. She is also grateful to Dr.Tsuyoshi Inoue, Dr. Nobuko Kanehisa, and Dr. Hiroyoshi Matsumura for their stimulating discussion and warm encouragement . The author acknowledges to Professor Takumi Ohshima and Dr. Masashi Hamaguchi and Dr. Ken Kokubo at Oshima Laboraotry.

The author greatly thanks Professor Fumio Toda(Okayama university of Science) and Dr. Koichi Tanaka(Ehime University) for their useful suggestions and hearty advices . She also acknowledges to Dr. Yukio Yamamoto (The Institute of Scientific Industrial Research) for his fruitful discussions and useful suggestions. She is also grateful to Dr. Kazuki Sada and all other menbers in the research group of Professor Mikiji Miyata for their helpful suggestions and discussions .

The author would like to thank all Professors in the chemcal department of Osaka University, for their kindly helps.

The author wish to thank Professor Kiichi Takemoto(Ryukoku University) , Professor Koichi Kondo(Ritsumeikan University), Dr.Takehiko Wada for their guidances and supports in Takemoto Laboratory for a long time.

The author is also grateful to Dr. Norimitsu Tohnai for his continuous warm encouragement and friendship. Special thanks are given to author's co-worker, Mr. Nobuyoshi Yasui.

The author is also thankful to her co-workers , Mr. Yoshiyuki Shibamoto, Ms.Akiko Nishi-Sakai, Mr.Tatsuya Maruo, Mr. Kyoichi Morioka , Mr.Yukinori Yamauchi, Ms.Emi Tani, Mr.Fujinori Satoh for their helpful suggestions and hearty encouragement and friendship.

Grateful acknowledgement are made to many graduates, Dr. Genji Kurisu, Dr. Naoki Shibata, Dr. Hajime Sugawara, Dr.Hiroshi Hashimoto, Ms. Mika Terada, Mr. Shunsuke Shirakata,

Mr.Yoichi Miyamoto and all other members of the research group of Professor Yasushi Kai for their kind assistance.Sincere thanks are also due to all her friends for their encouragement and helps.

The author wish to express her thanks to her parents (Mr. Masao Mochizuki and Ms. Setsuko Mochizuki, Mr. Satoru Harada and Ms. Masae Harada), sisters (Ms.Yuko Mochizuki, Ms. Michiko Harada, Mr. Kouji Harada and Ms.Yuko Harada) for their understanding on her works and hearty encouragement.

Finally, the author is specially thankful to her husband, Mr. Nobuyuki Harada and her beloved children , Mr. Akinobu Harada and Ms. Asako Harada for their understanding , encouragement, supports and tenderness .

July 2001

Mochizuki Eiko